



**Technical
University
of Lisbon
PORTUGAL**



**Technical
University
of Warsaw
POLAND**

**COMBINING ADAPTIVE ANTENNAS AT BOTH
THE BASE STATION AND THE MOBILE TERMINAL
IN UMTS**

Maciej Odzinkowski

**DEGREE IN ELECTRICAL AND COMPUTER ENGINEERING
Graduation Report**

Supervisor: Prof. Luis M. Correia

October 2004

Under the supervision of:

Prof. Luis M. Correia

Department of Electrical and Computer Engineering
Instituto Superior Técnico, Technical University of Lisbon
Portugal

To my dear parents

Acknowledgments

First of all, I would like to thank my supervisor, Professor Luis M. Correia for giving me opportunity to work in his team, for his trust, patience and sharing his professional and human wisdom.

Thanks to João Gil for his help, sharing his work, knowledge, and for his professional advice that helped to achieve my goal.

Thanks to the Growing Group colleagues, especially to Pedro, for the exchange of professional experiences approaching different technical subjects; to my Lab's colleagues, Daniel, João and Francisco, for surrounded me with friendly and nice atmosphere.

I want to thank Monika for love, patience, trust, and for supporting me in every moment in my life.

I would like to thank my family for love, belief, support and everything that they have done for me, not only during this time, but also during all my life.

Thanks to Dr. Jacek Jarkowski and Dr. Tomasz Kosiło for making this study possible, and for the help in arranging my Socrates – Erasmus scholarship.

Finally, I would like to thank the “Foundation for the Development of Radiocommunication and Multimedia Technologies” for supporting this scholarship, which made this study possible.

Thanks to all other people that I met or already known, but I didn't mention by name.

Abstract

In this thesis, Adaptive Beamforming at both the base station and the mobile terminal in the UMTS – TDD mode, in macro- and micro-cell environments has been studied. The beamforming is controlled by an adaptive, Conjugate Gradient algorithm. Two types of antenna arrays are considered: uniform linear array and uniform circular one.

A Wideband Directional Channel Model, based on the Geometrically Based Single Bounce Model, has been implemented to simulate specific macro- and micro-cell propagation scenarios.

The target of this work is to simulate and analyse what scenario parameters, particularly channel parameters, are the most important in terms of beamforming, and which order of gains and signal to interference-plus-noise ratio one can expect. The simulation environment has been prepared in MATLAB[®] for the UMTS – TDD mode.

It has been verified that the distance between mobile terminal and base station has an impact on the beamforming. By varying the distance, the beamforming gain takes values in the order of 10-20 dB, for macro- and micro-cells.

Keywords

UMTS, Beamforming, Conjugate Gradient, Wideband Directional Channel Model.

Abstrakt

Przedmiotem niniejszej pracy jest adaptacyjne formowanie wiązki antenowej zarówno w stacji bazowej jak i w terminalu mobilnym pracujących w systemie UMTS – TDD, zarówno dla środowiska makro- i mikro-komórkowego. Formowanie wiązki antenowej jest kontrolowane przez adaptacyjny, Conjugate Gradient algorytm. Uwzględniono dwa typy szyków antenowych: jednorodny liniowy oraz jednorodny kołowy.

Wideband Directional Channel Model, bazujący na Geometrically Based Single Bounce Model, został zaimplementowany do symulowania specyficznych makro- i mikro-komórkowych scenariuszy propagacyjnych.

Celem pracy jest wykonanie symulacji i analizowanie które parametry scenariuszy, szczególnie parametry kanału są najbardziej istotne w warunkach formowania wiązki, oraz jaki poziom mocy i stosunek sygnału do interferencji i szumu można oczekiwać. Środowisko symulacyjne zostało przygotowane za pomocą programu MATLAB® dla systemu UMTS – TDD.

Udowodniono że dystans pomiędzy terminalem mobilnym a stacją bazową ma wpływ na formowanie wiązki. Zmieniając dystans, moc formowania wiązki zmienia się od 10 do 20 dB, zarówno dla makro- jak i mikro-komórek.

Słowa kluczowe

UMTS, formowanie wiązki, Conjugate Gradient, Wideband Directional Channel Model.

Table of Contents

| | |
|--|-------------|
| Acknowledgments | v |
| Abstract | vii |
| Abstrakt | viii |
| Table of Contents | ix |
| List of Figures | xi |
| List of Tables | xiii |
| List of Acronyms | xiv |
| List of Symbols | xvii |
| 1 Introduction | 1 |
| 2 Theoretical Aspects | 5 |
| 2.1 UMTS Description | 5 |
| 2.1.1 UMTS Architecture | 5 |
| 2.1.2 Wideband Code Division Multiple Access | 7 |
| 2.2 Smart Antennas and Adaptive Algorithms | 12 |
| 2.2.1 Key Features of Smart Antennas | 12 |
| 2.2.2 Main Classes of Smart Antennas..... | 13 |
| 2.2.3 Main Adaptive Beamforming Algorithms..... | 15 |
| 2.2.4 Conjugate Gradient Algorithm..... | 18 |
| 2.3 Antenna Arrays | 19 |
| 2.4 Wideband Propagation Channels | 21 |
| 2.4.1 Introduction..... | 21 |
| 2.4.2 Geometrically Based Single Bounce Models | 22 |
| 2.4.3 Wideband Directional Channel Models..... | 24 |
| 3 Implementation | 27 |
| 3.1 General Concept of Performing the Simulation | 27 |
| 3.2 Multi-user Scenarios | 33 |

| | | |
|----------|--|-----------|
| 4 | Analysis of Results..... | 37 |
| 4.1 | Initial Considerations | 37 |
| 4.2 | Macro-cell Analysis | 39 |
| 4.3 | Micro-cell Analysis..... | 42 |
| 5 | Conclusions | 47 |
| | Annex A – Comparison of radiation patters | 49 |
| | Annex B – CG converges along the number of iteration..... | 55 |
| | References | 57 |

List of Figures

| | |
|--|----|
| Figure 2.1 – UMTS domains and network elements (extracted from [HoTo01]). | 5 |
| Figure 2.2 – UMTS network architecture (extracted from [KALN01]). | 6 |
| Figure 2.3 – Radio interface protocol architecture around the physical layer (extracted from [3GPP03a]). | 7 |
| Figure 2.4 – Spectrum allocations in Europe, Japan, Korea, and USA (extracted from [HoTo01]). | 8 |
| Figure 2.5 – Relation between spreading and scrambling (extracted from [HoTo01]). | 9 |
| Figure 2.6 – Code-tree for generation of Orthogonal Variable Spreading Factor (OVSF) codes (extracted from [3GPP03b]). | 10 |
| Figure 2.7 – Interference between MTs, between BSs, and between MT and BS. | 10 |
| Figure 2.8 – Intra-cell interference between several MTs and BS. | 11 |
| Figure 2.9 – Two smart antennas technologies (extracted from [LiRa99]). | 14 |
| Figure 2.10 – A baseband digital signal processing adaptive array structure (extracted from [LiRa99]). | 14 |
| Figure 2.11 – A generic adaptive beamforming system (extracted from [LiLo96]). | 15 |
| Figure 2.12 – Far-field geometry of M-element linear array of isotropic sources (extracted from [Szym02]). | 19 |
| Figure 2.13 – Geometry of an M-element circular array (extracted from [Szym02]). | 21 |
| Figure 2.14 – Geometry for the GBSBCM scattering region (extracted from [ZoMa00]). | 22 |
| Figure 2.15 – Geometry for the GBSBEM scattering region (extracted from [ZoMa00]). | 23 |
| Figure 2.16 – Cluster and scatterer distributions, indicating some single-bounce reflections (extracted from [GiCo03]). | 24 |
| Figure 3.1 – General concept of performing each beamforming simulations. | 28 |
| Figure 3.2 - General steps of performing each beamforming simulations. | 31 |
| Figure 3.3 – Simulation flowchart. | 32 |
| Figure 4.1 – Examples of BG evolution as a function of iteration number. | 37 |
| Figure 4.2 – Comparison between two independent groups of 300 channel realisations for scenario Sc#MaC_a. | 38 |
| Figure 4.3 – BG and SINR as a function of BS-MT distance for the 1 st step of beamforming; scenario Sc#MaC_a. | 40 |

| | |
|---|----|
| Figure 4.4 – BG and SINR as a function of BS-MT distance for the 2 nd step of beamforming; scenario Sc#MaC_a. | 40 |
| Figure 4.5 – BG and SINR as a function of BS-MT distance for the 3 rd step of beamforming; scenario Sc#MaC_a. | 41 |
| Figure 4.6 – Comparison of radiation patters for ULA and UCA, for 1500m BS-MT distance; scenario Sc#MaC_a. | 42 |
| Figure 4.7 – BG and SINR as a function of BS-MT distance for the 1 st step of beamforming; scenario Sc#MiC_a. | 43 |
| Figure 4.8 – BG and SINR as a function of BS-MT distance for the 2 nd step of beamforming; scenario Sc#MiC_a. | 43 |
| Figure 4.9 – BG and SINR as a function of BS-MT distance for the 3 rd step of beamforming; scenario Sc#MiC_a. | 44 |
| Figure 4.10 – Comparison of radiation patters for ULA and UCA, for 500m BS-MT distance; scenario Sc#MiC_a. | 45 |
| Figure A.1 – Comparison of radiation patterns for MaC, for BS-MT distance set to 1000 m; scenario Sc#MaC_a. | 49 |
| Figure A.2 – Comparison of radiation patterns for MaC, for BS-MT distance set to 1500 m; scenario Sc#MaC_a. | 50 |
| Figure A.3 – Comparison of radiation patterns for MaC, for BS-MT distance set to 2000 m; scenario Sc#MaC_a. | 51 |
| Figure A.4 – Comparison of radiation patterns for MiC, for BS-MT distance set to 200 m; scenario Sc#MiC_a. | 52 |
| Figure A.5 – Comparison of radiation patterns for MiC, for BS-MT distance set to 500 m; scenario Sc#MiC_a. | 53 |
| Figure A.6 – Comparison of radiation patterns for MiC, for BS-MT distance set to 1000 m; scenario Sc#MiC_a. | 54 |
| Figure B.1 – Comparison of CG converges along the number of iteration for MaC and MiC. | 55 |

List of Tables

| | |
|---|----|
| Table 2.1 – Main WCDMA parameters (extracted from [HoTo01])..... | 9 |
| Table 2.2 – Summary of optimum beamformers (extracted from [VeBu88]). | 16 |
| Table 3.1 – WDCM micro-cell scenarios..... | 35 |
| Table 3.2 – WDCM macro-cell scenarios..... | 36 |
| Table 4.1 – Simulation results for MaC; scenario Sc#MaC_a..... | 39 |
| Table 4.2 – Simulation results for MiC; scenario Sc#MiC_a..... | 42 |

List of Acronyms

| | |
|---------|---|
| 1G | First Generation |
| 2G | Second Generation |
| 3G | Third Generation |
| 3GPP | 3 rd Generation Partnership Project |
| AoA | Angle-of-Arrival |
| AF | Array Factor |
| ASILUM | Advanced Signal Processing Schemes for Link Capacity Increase in UMTS |
| BoD | Bandwidth on Demand |
| BG | Beamforming Gain |
| BS | Base Station |
| CDMA | Code Division Multiple Access |
| CG | Conjugate Gradient |
| CLPC | Closed Loop Power Control |
| CN | Core Network |
| CS | Circuit Switched |
| DCIR | Directional Channel Impulse Response |
| DesS | Desired Signal |
| DL | Downlink |
| DoA | Direction-of-Arrival |
| DS-CDMA | Direct Sequence Code Division Multiple Access |
| FDD | Frequency Division Duplex |
| FLAWS | Flexible Convergence of Wireless Standard and Services |
| GBSB | Geometrically Based Single Bounce |
| GBSBCM | Geometrically Based Single Bounce Circular Model |
| GBSBEM | Geometrically Based Single Bounce Elliptical Model |
| GGSN | Gateway GPRS Support Node |
| GMSC | Gateway MSC |
| GPS | Global Positioning System |
| GPRS | General Packet Radio Service |
| GSM | Global System for Mobile Communications |
| HLR | Home Location Register |

| | |
|---------|--|
| LCMV | Linear Constrained Minimum Variance |
| LLSE | Linear Least Squares Error |
| LMS | Least Mean Squares |
| LoS | Line of Sight |
| MaC | Macro Cell |
| MAC | Medium Access Control |
| Max SNR | Maximum Signal-to-Noise-Ratio |
| ME | Mobile Equipment |
| MGBSB | Modified Geometrically Based Single Bounce |
| MiC | Micro Cell |
| MMSE | Minimum Mean Square Error |
| MSC | Mobile services Switching Centre |
| MSCI | Multiple Sidelobe Canceller |
| MT | Mobile Terminal |
| NDesI | Non-Desired Interference |
| OLPC | Open Loop Power Control |
| OVSF | Orthogonal Variable Spreading Factor |
| PC | Power Control |
| PDF | Probability Density Function |
| PS | Packet Switched |
| QoS | Quality of Service |
| RF | Radio Frequency |
| RLC | Radio Link Control |
| RLS | Recursive Least Squares |
| RNC | Radio Network Controller |
| RNS | Radio Network Subsystem |
| RRC | Radio Resource Control |
| SA | Smart Antenna |
| SAP | Service Access Point |
| SDMA | Space Division Multiple Access |
| SF | Spreading Factor |
| SGSN | Serving GPRS Support Node |
| SIR | Signal-to-Interference Ratio |

| | |
|-------|--|
| SINR | Signal to Interference-plus-Noise Ratio |
| SMI | Sample Matrix Inversion |
| SNR | Signal-to-Noise Ratio |
| TDD | Time Division Duplex |
| ToA | Time-of-Arrival |
| UCA | Uniform Circular Array |
| UE | User Equipment |
| UMTS | Universal Mobile Telecommunications System |
| UL | Uplink |
| ULA | Uniform Linear Array |
| USIM | User Services Identity Module |
| UTRAN | Universal Terrestrial Radio Access Network |
| VLR | Visitor Location Register |
| WCDMA | Wideband Code Division Multiple Access |
| WDCM | Wideband Directional Channel Model |
| WDDCM | Wideband Double Directional Channel Model |

List of Symbols

| | |
|--------------------------|---|
| λ | wavelength |
| θ | azimuthal angle |
| ϕ | horizontal angle |
| ϕ_0 | MT angular position |
| ϕ_n | angular position of n^{th} element of UCA on x-y plane |
| τ | time delay |
| τ_{max} | maximum time delay |
| ψ_n | phase excitation (relative to the array to the centre) of the n^{th} element |
| b | cross-correlation vector between the input data and desired signal |
| c | speed of light |
| C_{ch} | channelisation code |
| d | desired/reference signal |
| d_e | distance between radiating elements at antennas array |
| d_T | distance between MT and BS |
| $G_{\text{beamforming}}$ | beamforming gain |
| G_p | processing gain |
| i | iteration index |
| K | number of concretisations |
| k | code number |
| L | number of MT-BS links |
| M | number of array elements |
| N | number of matrix elements |
| N_s | number of baseband signal samples |
| N_{th} | noise power |
| P_{DesS} | desired signal power |
| P_{NDesI} | non-desired interference powers |
| R | correlation matrix of the input data vector |
| r_a | antenna radius |
| r_{max} | radius of scatterers region |
| U | channel matrix |

w weights vector
x input signal vector
y output signal

1 Introduction

First Generation (1G) Systems started to be developed at the beginning of the 70's. It was the first step to create a uniform international system for mobile communications. This system did not succeed, because the terminals were big and expensive, and also technology was different in different countries. Then, in the 90's, Second Generation (2G) Systems evolved, and that brought more efficiency and accessibility for the majority of the public. In Europe, this 2G system is called Global System for Mobile Communications (GSM) and developed rapidly. After the success of GSM, people started working on new architectures to improve mobile communications. The objective is to provide services to every user, in every place of the world at all times. Many people are working on making it better and they want to provide a global mobility with a wide range of services including Internet, telephony, messaging and broadband data. This Third Generation (3G) System is called Universal Mobile Telecommunications System (UMTS), being designed to enable multimedia communication like images and video, and access to information and services on private and public networks with higher data rates.

UMTS introduced new requirements which are listed below [HoTo01]:

- bit rates up to 2 Mbps;
- variable bit rate to offer Bandwidth on Demand (BoD);
- multiplexing of services with different quality requirements on a single connection, e.g., speech, video and packet data;
- delay requirements from delay-sensitive real-time traffic to flexible best-effort packet data;
- quality requirements from 10% frame error rate to 10^{-6} bit error rate;
- coexistence of 2G and 3G systems and inter-system handover for coverage enhancements and load balancing;
- support of asymmetric uplink (UL) and downlink (DL) traffic, e.g., web browsing causes more loading to DL than to UL;
- high spectrum efficiency;
- coexistence of Frequency Division Duplex (FDD) and Time Division Duplex (TDD) modes.

In order to achieve and perform these requirements, *smart* and *intelligent* technologies started to play a major role in mobile wireless communications. Smart technologies are one of many ways to improve the system, at the antenna receiver, and at the baseband processing levels, to gain capacity, coverage or quality.

Using Smart Antennas (SAs) combined with adaptive algorithms to improve received, and transmitted signal quality, is one of the main task for further study, because of the many advantages that it can provide. Smart adaptive antennas play the role of surgically applying the best array pattern, either at the Base Station (BS) or at the Mobile Terminal (MT), according to their relative location, number, and channel conditions. The objective of their use is to improve system capacity. It is not new that the use of antenna arrays inherently provides processing gain to improve BS range and coverage but, most importantly, such systems render Signal to Interference-plus-Noise Ratio (SINR) improvement, especially where user densities and traffic load tend to be large.

In UMTS, being a Wideband Code Division Multiple Access (WCDMA) system, the limitation is at the noise level, or to be more precise at SINR. For this reason, it is important to gain as much as possible from the signals that one wants to receive/transmit, and suppress or cancel the ones that one does not need.

The target of this work is to simulate and analyse what scenario parameters, particularly channel parameters, are the most important in terms of beamforming, and which order of gains one can expect.

It is important to mention that the whole work is fundamentally based on simulations, making use of a channel model and important assumptions. UMTS has been assumed as the system that will be used in simulations. As a result of a closer analysis of this system, some issues were identified as important: one has to use proper frequencies, codes, and power control mechanisms. After that, an important issue is to learn about the transmission medium, namely radio channel, which is a key issue for the design and implementation. Already knowing the system and performance, one can analyse the beamforming, i.e., the proper type of antennas, and algorithms, depending on the available input signals. Finally, one has to study how to feed the antenna, and the overall view is complete.

The work presented in this thesis explores the utilisation of Adaptive Beamforming for both the BS and the MT in the UMTS – TDD mode in macro- and micro-cell environments for some specific scenarios. The simulation environment has been prepared in MATLAB[®], and a number of simulations have been performed. General conclusions are

drawn on the basis of obtained results, main features, and characteristics of used scenarios have been identified, as well as importance or triviality of parameters used.

It should be mentioned that the work presented in this thesis has been based on work made for UMTS – TDD and UMTS – FDD, concerning beamforming at the BS, [Gil04], [Olej02], [Szym02]. The work has been enlarged by new elements in order to apply to the UMTS – TDD mode. Filtering and multiplying responses from the propagation channel with antennas array pattern has been added to obtain a beamforming at both the BS and the MT. Additionally, simulations for macro- and micro-cell environments have been made and presented.

This thesis is organised as follows. Chapter 2 describes theoretical aspects of all needed elements, starting from the general principles of UMTS, across smart antennas, adaptive algorithms and theory of antenna arrays, and finishing with wideband propagation channels. Chapter 3 contains all issues related with the implementation of consecutive parties of the system for simulation; one can also find here a description of the analysis procedure and scenarios used. Chapter 4 brings an analysis of obtained results divided in macro- and micro-cells analysis, comparison of both, and some general observations. Finally, in Chapter 5, conclusions are drawn, with a summary of the whole work, and proposals for future work are presented. In Annexes, one can find the CG convergence along the number of iteration, and antenna's radiation pattern for each of scenarios.

Innovative aspects of the work constitute the utilisation of adaptive beamforming for both the BS and the MT in UMTS – TDD. The beamforming is generated at the MT with the beamformer at the BS, and also the opposite situations have been considered, when the beamforming is generated at the BS with the beamformer at the MT. It shows the dependency of BS-MT beamforming all together, and describes the whole process of performing the beamforming at both sides.

2 Theoretical Aspects

2.1 UMTS Description

2.1.1 UMTS Architecture

This section gives an overall view of the 3G system architecture, including some information about the logical network elements and the interfaces.

UMTS consists of three interacting domains: the User Equipment (UE) Domain, UMTS Terrestrial Radio Access Network (UTRAN) Domain and Core Network (CN) Domain. The high-level system architecture with network elements is shown in Figure 2.1.

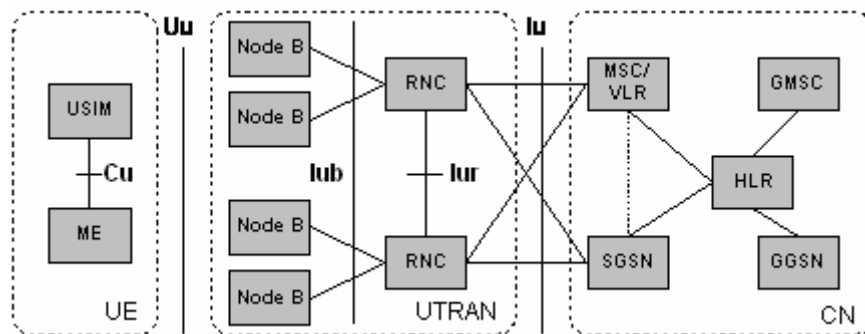


Figure 2.1 – UMTS domains and network elements (extracted from [HoTo01]).

The UE Domain is responsible for access to UMTS services, which is done via a radio interface. It consists of the UMTS Subscriber Identity Module (USIM) and the Mobile Equipment (ME). The ME is the radio terminal used for radio communication over the “Uu” interface. The USIM performs data and procedures for subscriber identity, and some information that is needed at the terminal, and these functions are embedded in a smartcard. The interface between ME and UMTS Subscriber Identity Module is designated by the “Cu” interface.

The UTRAN Domain provides the air interface access. It is divided into Radio Network Subsystems (RNSs). Each RNS contains the radio network element Node-B, or Base Station (BS), and control equipment Radio Network Controller (RNC). The interface between the Node-B and the RNC is the ‘Iub’ interface. Between RNSs there is the ‘Iur’ interface.

The CN Domain function is to provide routing, switching and data connections to external networks. The basic CN architecture for UMTS is based on the GSM network with

GPRS, but all elements have to be modified for UMTS operation and services. The CN consists of the Mobile services Switching Centre (MSC), Visitor Location Register (VLR) and Gateway MSC (GMSC). These elements are Circuit Switched (CS) domains, but the Core Network Domain is divided in Packet Switched (PS) domains as well: Serving GPRS Support Node (SGSN) and Gateway GPRS Support Node (GGSN). The CN also consists of the Home Location Register (HLR), which is shared by both CS and PS domains.

The interface between the logical network elements, UE and UTRAN, is the ‘Uu’ interface, which is the WCDMA radio interface. The other interface is the ‘Iu’ located between the UTRAN and CN.

The UMTS network architecture is shown in Figure 2.2.

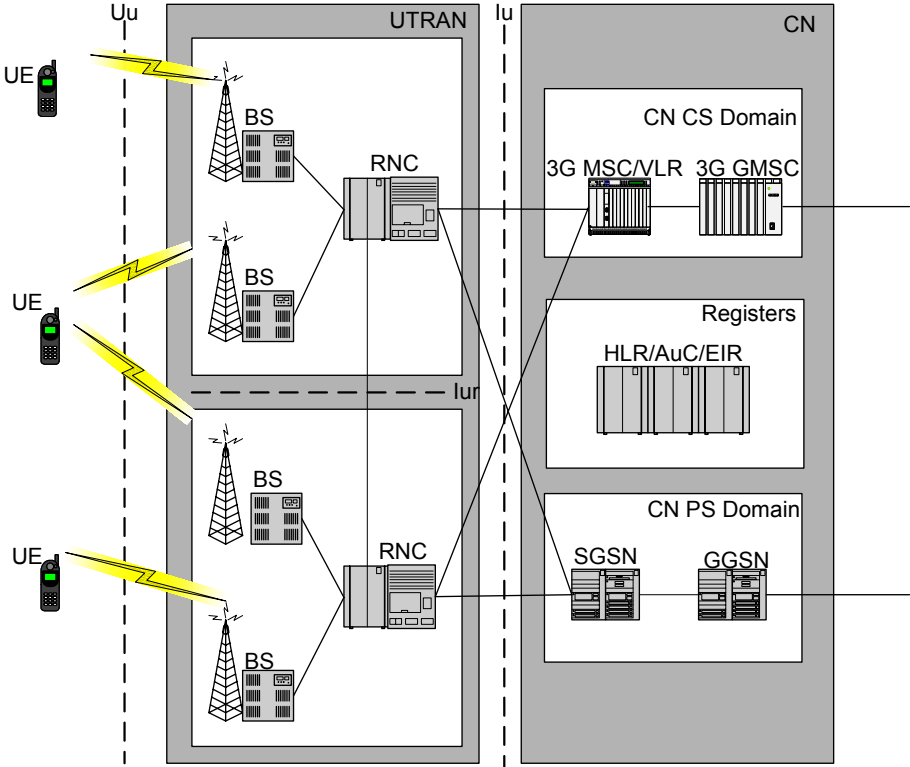


Figure 2.2 – UMTS network architecture (extracted from [KALN01]).

The radio interface protocol architecture around the physical layer architecture is shown in Figure 2.3. The radio interface consists of Layers 1, 2 and 3. In UMTS there are three types of channels related with the layer structure of the system [3GPP03a]: physical channels, logical channels and transport channels. The physical layer interfaces the Medium Access Control (MAC) sub-layer of Layer 2 and the Radio Resource Control (RRC) Layer of Layer 3. The circles between different layer/sub-layers indicate Service Access Points

(SAPs). The physical layer offers services via transport channels to the MAC, characterised by how the information is transferred over the radio interface.

The MAC layer offers different Logical channels to the Radio Link Control (RLC) sub-layer of Layer 2. The logical channels are characterised by the type of information transferred.

Physical channels are defined in the physical layer. There are two duplex modes: Frequency Division Duplex (FDD) and Time Division Duplex (TDD). In the FDD mode a physical channel is characterised by the code, frequency and in the UL the relative phase (I/Q). In the TDD mode the physical channels is also characterised by the timeslot. The physical layer is controlled by RRC.

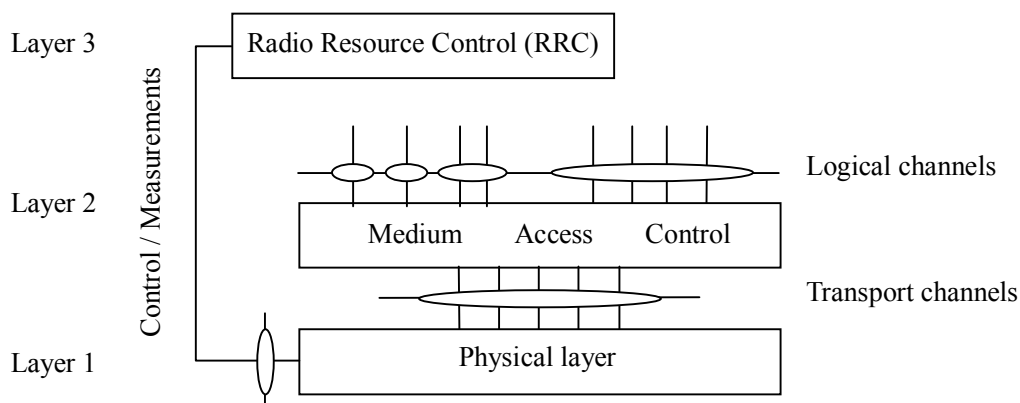


Figure 2.3 – Radio interface protocol architecture around the physical layer (extracted from [3GPP03a]).

2.1.2 Wideband Code Division Multiple Access

Wideband Code Division Multiple Access (WCDMA) is the radio interface, which is implemented in UMTS. WCDMA is a wideband Direct-Sequence Code Division Multiple Access (DS-SS-CDMA) system, which means that user information bits are spread over a wide bandwidth by multiplying the user data with quasi-random bits (called chips) derived from Code Division Multiple Access (CDMA) spreading codes [HoTo01]. The new requirements of 3G systems, as described in Chapter 1, are supported. The larger bandwidth of 5 MHz is needed to support higher bit rates. WCDMA improves the DL capacity to support the asymmetric capacity requirements between DL and UL.

WCDMA supports two basic modes of operation: FDD and TDD. For FDD, two separated 5 MHz radio bands for the UL and DL transmissions are required. For TDD, a single 5 MHz band is time-shared between UL and DL. TDD is used on an unpaired band,

while the FDD system requires a pair of bands. FDD has one chip-rate option, the 3.84 Mcps, whereas TDD has two options, the 3.84 Mcps and the 1.28 Mcps ones.

UMTS frequency bandwidth is allocated at around 2 GHz. In Europe, UMTS bands will be available in two groups. The first one will be available for WCDMA FDD and the second one for WCDMA TDD. The available frequency bands are:

- FDD (paired bands):
 - 1920 - 1980 MHz (UL)
 - 2110 - 2170 MHz (DL)
- TDD (unpaired bands):
 - 1900 - 1920 MHz
 - 2010 - 2025 MHz } (UL and DL)

12 radio channels are available for FDD, and 7 for TDD.

The spectrum allocation is shown in Figure 2.4.

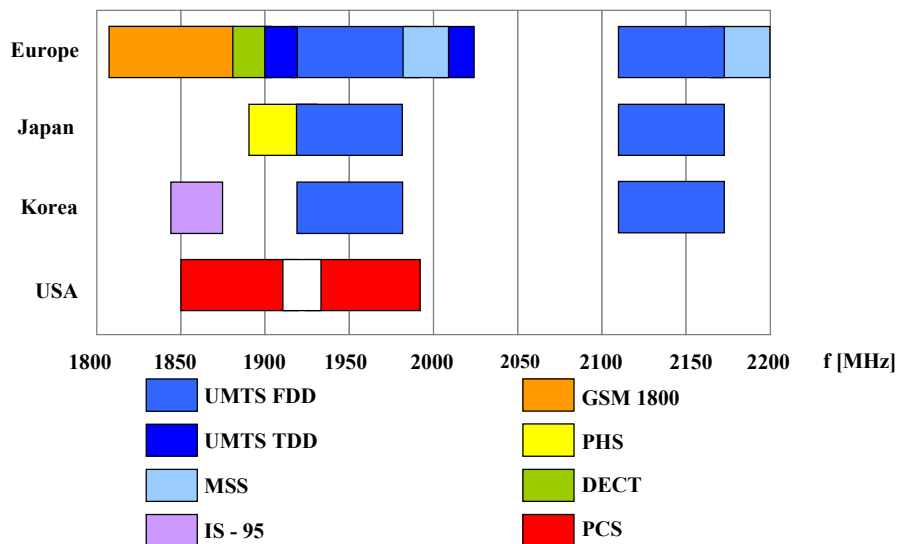


Figure 2.4 – Spectrum allocations in Europe, Japan, Korea, and USA (extracted from [HoTo01]).

WCDMA supports variable bit rate to offer BoD and 10 ms radio frame. In TDD, a 10 ms radio frame is divided into 15 timeslots each of 2560 chips at the chip rate 3.84 Mcps. Each of the 15 timeslots within a frame is allocated to either UL or DL. For the 1.28 Mcps TDD option, a 10 ms radio frame is divided into two 5 ms sub-frame. In each sub-frame, there are 7 normal time slots and 3 special time slots [3GPP03a].

There is no requirement for a global time reference, such as a Global Positioning System (GPS) because WCDMA supports the operation of asynchronous BSs. WCDMA

employs coherent detection on UL and DL based on the use of pilot symbols or common pilot. The use of coherent detection is new for public CDMA systems, and will result in an overall increase of coverage and capacity on the UL.

Table 2.1 shows the main parameters of WCDMA.

Table 2.1 – Main WCDMA parameters (extracted from [HoTo01]).

| | |
|-------------------------------------|---|
| Multiple access method | DS-CDMA |
| Duplexing method | FDD / TDD |
| Base station synchronization | Asynchronous operation |
| Chip rate | 3.84 Mcps |
| Frame length | 10 ms |
| Service multiplexing | Multiple service with different quality of service requirements multiplexed on one connection |
| Multirate concept | Variable spreading factor and multicode |
| Detection | Coherent using pilot symbols or common pilot |
| Multiuser detection, smart antennas | Supported by the standard, optional in the implementation |

In WCDMA system, there are two types of operations performed in the code domain: spreading/channelisation and scrambling [HoTo01]. The spreading operation transforms every data symbol into a number of chips, thus, increasing the bandwidth of the signal. Spreading/channelisation codes are used to separate transmissions from a single source, i.e., DL connections within one cell and the dedicated physical channel in the UL from one terminal. In addition to spreading, part of the process in the transmitter is the scrambling operation, which is applied to the spread signal. Scrambling is needed to separate BSs or UEs from each other. This operation in a code domain does not change the signal bandwidth, but only separates the signal from different sources, i.e., for FDD it separates different cells in DL and different terminals in UL direction, whereas for TDD scrambling codes separates cells. The relation of the chip rate in the channel to spreading and scrambling is shown in Figure 2.5.

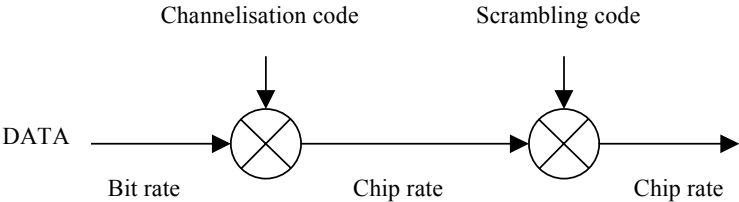


Figure 2.5 – Relation between spreading and scrambling (extracted from [HoTo01]).

The channelisation codes are Orthogonal Variable Spreading Factor (OVSF) ones. The OVSF codes can be defined using the code tree of Figure 2.6 [3GPP03b]. The channelisation codes are uniquely described as $C_{ch,SF,k}$; the number of chips per data symbol is called the Spreading Factor (SF), and k is the code number; $0 \leq k \leq SF-1$.

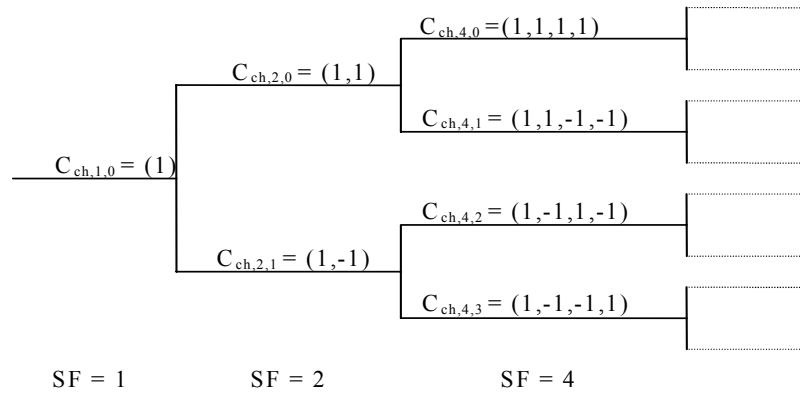


Figure 2.6 – Code-tree for generation of Orthogonal Variable Spreading Factor (OVSF) codes (extracted from [3GPP03b]).

In the TDD mode, the signal in the UL and DL transmissions (the same frequency band) can interfere with each other. The BSs have to be synchronised to each other at the frame level to control this interference. In FDD, between UL and DL, interference is completely avoided by the duplex separation of 190 MHz. There is interference among MTs, among BSs, among MT and BS. Figure 2.7 shows these interference interactions.

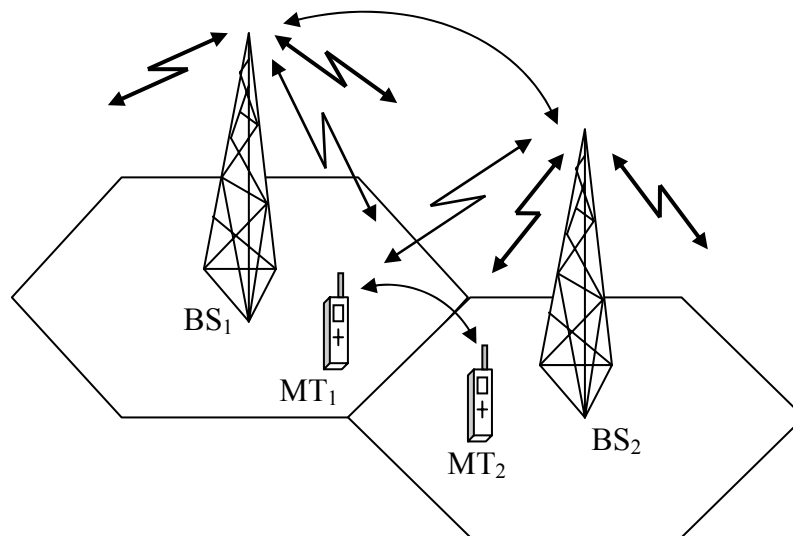


Figure 2.7 – Interference between MTs, between BSs, and between MT and BS.

Interference between MTs occurs if one of the MTs is transmitting and other MT is receiving simultaneously in adjacent cells in the same (or adjacent) frequency. There is also interference between MTs, especially at cell borders, where two operator’s mobiles are close to each other and transmitting with fairly high power.

Interference between BSs depends heavily on path loss between the two BSs and also depends on the BS locations. This interference occurs if one of the BSs is transmitting and other BS is receiving in adjacent cells in the same (or adjacent) frequency. The network planning has to be controlled to avoid this interference.

There is also interference between TDD and FDD, because the spectrum allocations of the lower TDD band and the FDD UL band, is located at 1920 MHz, but this interference are not considered in this work.

Inter-cell interference occurs between MTs and BSs within other cells, whereas within one cell intra-cell interference occurs between several MTs and BS. This work will be dealing with intra-cellular interference in the TDD mode. Figure 2.8 generally exemplifies a simple intra-cell interference situation that is at stake, but it is only refer to a single slot.

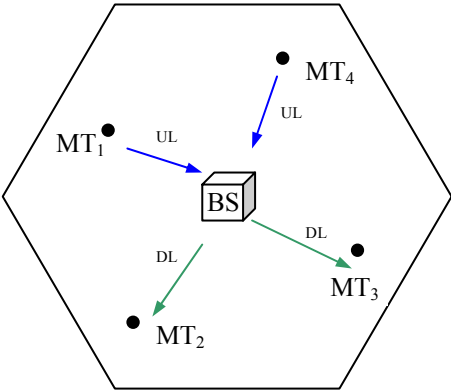


Figure 2.8 – Intra-cell interference between several MTs and BS

At MT₂, which is receiving signals from the BS, there is interference from transmitting MTs, MT₁ and MT₄, and from the BS-MT₃ link. At MT₃, which is also at DL, the same type of interference is achieved, i.e., at MT₃ there is interference from MT₁ and MT₄, and from the BS-MT₂ link. At MT₁ and MT₄ there is no interference for the corresponding time-slot. Due to these, intra-cell UL interference occurs at the BS, while there is no DL interference. At the BS, in respect to the MT₁-BS link there is interference from the BS-MT₄ link. Oppositely, at the BS relatively to the MT₄-BS link, there is interference from the BS-MT₁ link.

Besides the interference issue, Power Control (PC) is an important aspect in WCDMA and is needed to keep the interference levels at minimum in the radio interface and also to supply the required Quality of Service (QoS). In the DL, PC is used to minimise the interference to other cells and compensating for other cells interference. In the UL, an important problem that PC avoids is the *near-far effect*. In near-far situations, the signal of the MT that is close to the serving BS may dominate over the signal of the MTs that are far away from the same BS. PC avoids this problem, by making the transmission power level received from all terminals as equal and low as possible at the home cell, for the same QoS [Szym02].

In UMTS, PC has two types of loops, Open Loop Power Control (OLPC) and Closed Loop Power Control (CLPC). OLPC is used to adjust the output power of the received signal level from the BS to a specific value. It is used for setting initial transmission powers when the MT is connecting to the network. CLPC consists of two different loops: Outer Loop Power Control and Inner Loop Power Control. Inner Loop Power Control is the fastest loop in WCDMA power control mechanism, which is called Fast Closed Loop Power Control. Outer loop power control is used to maintain the required QoS, while using as low power as possible, whereas Inner Loop Power Control is used to keep the received Signal-to-Interference Ratio (SIR) at a given target and also to command the MT to increase or decrease its transmission power, with a cycle of 1.5 kHz, by 1, 2 or 3 dB step-sizes [HoTo01].

2.2 Smart Antennas and Adaptive Algorithms

2.2.1 Key Features of Smart Antennas

This section presents key features of smart antennas, including switched beam system and adaptive antenna concepts, especially focusing on adaptive beamforming algorithms.

Smart Antennas (SAs) are a new technology for the application in wireless systems. These, most often, use a fixed set of antenna elements in an array, and offer a broad range of ways to improve wireless system performance. The signal from these antenna elements are combined to form a movable beam pattern that can be steered. Most simplistically, a beam may be pointed to the desired direction that tracks mobile units as they move, using either digital signal processing, or Radio Frequency (RF) hardware. SA systems contribute to minimising the impact of noise and interference for each MT and BS. In general, SAs have

the potential to provide enhanced range and reduced infrastructure costs in early deployments, and increased system capacity [LiRa99]:

- SAs provide enhanced coverage through range extension, hole filling, and better building penetration. Given the same transmitter power output at the BS and MT, SAs can provide range extension by increasing the gain of the BS antenna.
- In early deployment, in order to meet initial coverage requirements, a number of BSs must be installed without customer revenue to support these BSs. SAs can ease this problem by allowing larger early cell sizes.
- SAs provide robustness to system perturbations and reduced sensitivity to non-ideal behavior. CDMA systems require PC to ensure that all of the signals arriving at a BS are at approximately the same power level. SAs help to isolate the UL signals from different users, reducing PC requirements or mitigating the impact of imperfect PC.
- Link quality can be improved through multipath management, i.e., since multipath in radio channels can result in fading or time dispersion, SAs help to mitigate the impact of multipath or even exploit the diversity inherent in multipath.
- SAs can help to improve system capacity. In CDMA systems, if SAs are used to allow subscribers to transmit less power for each link, then the Multiple Access Interference is reduced, which increases the number of simultaneous subscribers that can be supported in each cell.
- SAs can also be used to spatially separate signals, allowing different subscribers to share the same spectral resources, provided that they are spatially separable at the BS. Space Division Multiple Access (SDMA) allows multiple users to operate in the same cell, on the same frequency/time slot provided, using the SA to separate the signals.

2.2.2 Main Classes of Smart Antennas

SAs systems can include features of either adaptive antenna or switched beam technologies [LiRa99]. These two SA technologies are shown in Figure 2.9. Switched beam systems use a number of fixed beams at an antenna site. The receiver or transmitter chooses the best beam, i.e., the beam that provides the greatest signal performance and interference reduction, as it is shown in Figure 2.9a. Switched beam systems offer worse performance than adaptive antenna systems in spite of being of much simpler implementation. This work will be dealing with adaptive antennas. An adaptive antenna is an array of antennas, with a pattern

that is dynamically adjusted in terms of noise, interference, and multipath. As it is shown in Figure 2.9b, an adaptive antenna can adjust its whole antenna pattern to enhance the desired signal, minimise interference, and collect correlated multipath power.

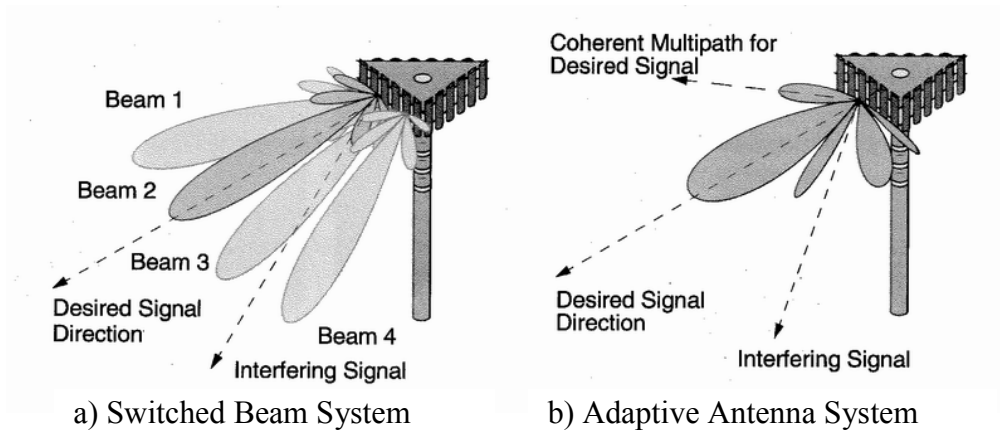


Figure 2.9 – Two smart antennas technologies (extracted from [LiRa99]).

In a baseband digital signal processing adaptive array, as it is exemplified in Figure 2.10, the weight vector $w_{k,i}$ is adjusted, or adapted, to maximise the quality of the signal that is available to the demodulator, for signal k at time index i . An estimate or replica of the desired signal for the i^{th} user at the array output, is represented by d_i .

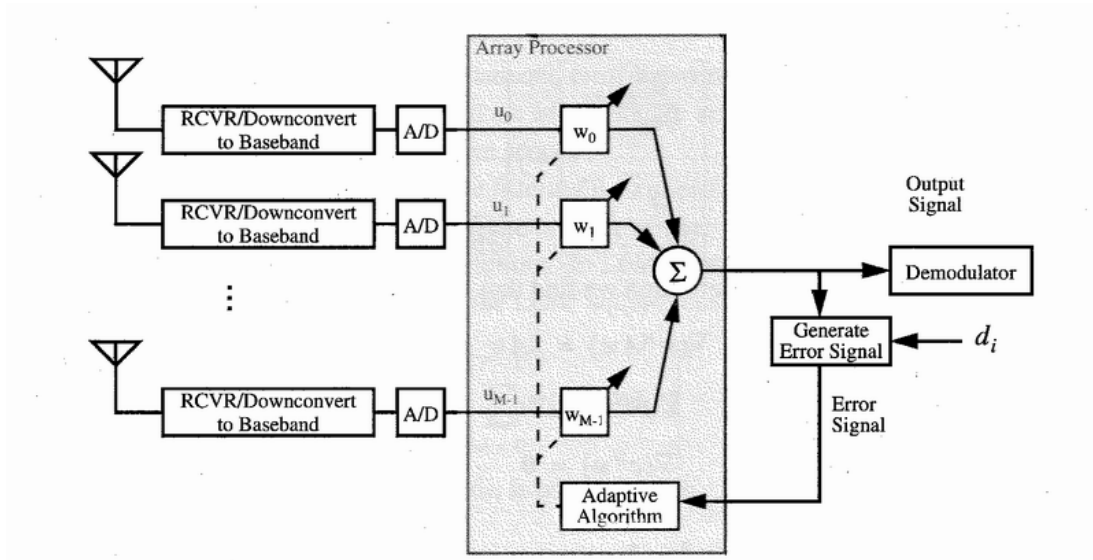


Figure 2.10 – A baseband digital signal processing adaptive array structure (extracted from [LiRa99]).

2.2.3 Main Adaptive Beamforming Algorithms

A generic non-blind adaptive beamforming system is shown in Figure 2.11. The selection of the weight vector \mathbf{w} is based on the signal vector $\mathbf{x}(t)$ received at the array and reference signal if such signal is required, $d^*(t)$. The objective of beamforming is to optimise the beamformer response with respect to a prescribed criterion, so that the output $y(t)$ contains minimal contribution from noise and interference.

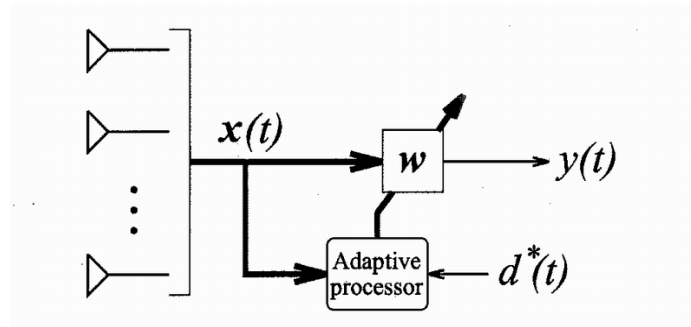


Figure 2.11 – A generic adaptive beamforming system (extracted from [LiLo96]).

There are a number of criteria for choosing the optimum weights [LiLo96]:

- Minimum Mean-Square Error (MMSE) attempts to minimise the difference between the array output and some desired signal.
- Maximum Signal-to-Noise Ratio (Max SNR) maximises the actual signal-to-noise ratio at the array output.
- Linear Constrained Minimum Variance (LCMV) minimises the variance at the output of the array.
- Multiple Sidelobe Canceller (MSCI), which goal is to choose the auxiliary channel weights to cancel the main channel interference component.

The selection of a criterion is not critically important in terms of performance, but it is important in terms of what information about the incoming signal is available [Szym02]. Depending on how the weights are chosen, the beamforming is divided between data independent or statistically optimum [VeBu88]. In a data independent, the weights do not depend on the array data and are chosen to present a specified response for all signal/interference scenarios. In a statistically optimum beamforming the weights are chosen based on the statistics of the data received at the array, to “optimise” the array response, i.e., the beamformer output contains minimal contributions due to noise and signal arriving from different directions than the desired signal. Table 2.2 summarises their main characteristics.

The selection of adaptive algorithms for obtaining adaptive weights is highly important, in that it determines both the speed of convergence and hardware complexity required to algorithm implementation. The simplest optimal beamforming technique is the MSC1 approach, but it requires absence of desired signal from auxiliary channels for weight determination. The Max SNR approach, which maximises SNR in the array output, and the LCMV approach are two techniques that require knowledge of Direction-of-Arrival (DoA) of the desired signal, which is not typically known in mobile and wireless systems. The MMSE approach attempts to minimise the difference between array output and some desired signal.

Table 2.2 – Summary of optimum beamformers (extracted from [VeBu88]).

| Type | MSC1 | MMSE | Max SNR | LCMV |
|-----------------|--|--|--|---|
| Inputs | \mathbf{x}_a – auxiliary data \mathbf{y}_m – primary data | \mathbf{x} – array data \mathbf{y}_d – desired signal | $\mathbf{x}=\mathbf{s}+\mathbf{n}$ \mathbf{s} – signal component \mathbf{n} – noise component | \mathbf{x} – array data \mathbf{C} – constraint matrix \mathbf{f} – response vector |
| Output | $\mathbf{y}=\mathbf{y}_m-\mathbf{w}_a^H\mathbf{x}_a$ \mathbf{w}_a – auxiliary weight vector | $\mathbf{y}=\mathbf{w}^H\mathbf{x}$ \mathbf{w} – weight vector | $\mathbf{y}=\mathbf{w}^H\mathbf{x}$ \mathbf{w} – weight vector | $\mathbf{y}=\mathbf{w}^H\mathbf{x}$ \mathbf{w} – weight vector |
| Criterion | $\min_{\mathbf{w}} E\left\{\left \mathbf{y}_m-\mathbf{w}_a^H\mathbf{x}_a\right ^2\right\}$ | $\min_{\mathbf{w}} E\left\{\left \mathbf{y}-\mathbf{y}_d\right ^2\right\}$ | $\max_{\mathbf{w}} \frac{\mathbf{w}^H\mathbf{R}_s\mathbf{w}}{\mathbf{w}^H\mathbf{R}_n\mathbf{w}}$ | $\min_{\mathbf{w}}\left\{\mathbf{w}^H\mathbf{R}_x\mathbf{w}\right\}\text{s.t.}\mathbf{C}^H\mathbf{w}=\mathbf{f}$ |
| Optimum Weights | $\mathbf{w}=\mathbf{R}_a^{-1}\mathbf{r}_{ma}$ where: $\mathbf{r}_{ma}=\mathbf{E}\left\{\mathbf{x}_a\mathbf{y}_m^*\right\}$ $\mathbf{R}_a=\mathbf{E}\left\{\mathbf{x}_a\mathbf{x}_a^H\right\}$ | $\mathbf{w}=\mathbf{R}_x^{-1}\mathbf{r}_{xd}$ where: $\mathbf{r}_{xd}=\mathbf{E}\left\{\mathbf{x}\mathbf{y}_d^*\right\}$ $\mathbf{R}_x=\mathbf{E}\left\{\mathbf{x}\mathbf{x}^H\right\}$ | $\mathbf{R}_n^{-1}\mathbf{R}_s\mathbf{w}=\lambda_{\max}\mathbf{w}$ where: $\mathbf{R}_s=\mathbf{E}\left\{\mathbf{s}\mathbf{s}^H\right\}$ $\mathbf{R}_n=\mathbf{E}\left\{\mathbf{n}\mathbf{n}^H\right\}$ | $\mathbf{w}=\mathbf{R}_x^{-1}\mathbf{C}\left[\mathbf{C}^H\mathbf{R}_x^{-1}\mathbf{C}\right]^{-1}\mathbf{f}$ where: $\mathbf{R}_x=\mathbf{E}\left\{\mathbf{x}\mathbf{x}^H\right\}$ |
| Advantages | Simple | Direction of desired signal can be unknown | True maximisation of SNR | Flexible and general constrains |
| Disadvantages | Requires absence of desired signal from auxiliary channels for weight determination | Must generate reference signal | Must know \mathbf{R}_s and \mathbf{R}_n , solve generalised eigen-problem for weights; DoA of desired signal must be known | Computation of constrained weight vector; must know DoA of desired component |

An explicit reference signal is helpful in a communications system, for less complexity, high accuracy, and fast convergence. Algorithms that require reference signal sequence are referred to as *non-blind algorithms*. Non-blind algorithms are characterised by fast convergence and easy to implement, although these require a reference signal. In the case where a reference signal is not available, *blind adaptive algorithms* have to be used. These algorithms are not mentioned at this work, because for the WCDMA system, non-blind adaptive beamforming may be applied. The spreading/channelisation code, performed in the WCDMA system, can be used as reference for beamforming.

The common adaptive algorithms that have been investigated for beamforming in mobile communications include the Least Mean Squares (LMS) algorithm, the Sample Matrix

Inversion (SMI) technique and Recursive Least Squares (RLS) algorithm [LiLo96]. The simplest algorithm to implement is the LMS one, but it has its drawbacks: the dynamic range over which it operates is quite limited. If dynamic range increases more than the permissible order, PC is required if the LMS algorithm is to be used. The SMI approach offers a relatively fast convergence rate, but in order to achieve it, the direct inversion of the covariance matrix should be employed. If we know a priori the desired and interference signal, then the covariance matrix could be evaluated and the optimal solution for the weights could be computed using SMI [LiLo96]. An important feature of the RLS Algorithm [LiLo96], [GiMC01] is that the inversion of covariance matrix is replaced at each step by a simple scalar division, and it reduces the computational complexity while maintaining a similar performance. The RLS approach offers an order of magnitude faster convergence rate than the LMS algorithm, provided that the signal-to-noise ratio is high.

There are other adaptive techniques, which have also been applied to beamforming in mobile communications. These techniques include the Conjugate Gradient (CG) method, the Linear Least Squares Error (LLSE) algorithm, the method based on rotational invariance, and the Hopfield neural network [LiLo96]. All these methods have been proposed to either improve the performance or level the shortcomings of the LMS, SMI, or RLS algorithms.

The mentioned algorithms, generally described in this subsection, are just examples of different approaches to the beamforming problem, because the variety of approaches is very rich. In the next section, the CG algorithm is described in more detail.

As results of dealing with adaptive beamforming algorithms, the objective is to calculate the Beamforming Gain (BG), and Signal to Interference-plus-Noise Ratio (SINR) for a single antenna's element and for each link.

The calculation of SINR for the l^{th} link follows, [Gil04]:

$$SINR^{(l)} = \frac{P_{DesS}^{(l)} \cdot G_p}{\sum_{l_T=1}^{L_T} P_{NDesI}^{(l)} + N}, \quad (2.1)$$

where:

- G_p – CDMA processing gain (equal to the spreading factor);
- P_{DesS} – Desired Signal (DesS) power;
- P_{NDesI} – Non-Desired Interference (NDesI) power;
- N – total noise power.

The l^{th} BG at the BS, $G_{\text{beamformer (BS)}}$, is defined as the SINR gain relative to the SINR achieved with a single omnidirectional antenna at the BS, for each of the L active links:

$$G_{\text{beamformer(BS)}}^{(l)} = \text{SINR}^{(l)} \Big|_{\text{beamformer}} - \text{SINR}^{(l)} \Big|_{\text{single (BS)}} \quad [\text{dB}], \quad (2.2)$$

whereas, the l^{th} BG at the MT, $G_{\text{beamformer (MT)}}$, is defined as the SINR gain relative to the SINR achieved with a single omnidirectional antenna at the MT, for each of the L active links:

$$G_{\text{beamformer(MT)}}^{(l)} = \text{SINR}^{(l)} \Big|_{\text{beamformer}} - \text{SINR}^{(l)} \Big|_{\text{single (MT)}} \quad [\text{dB}]. \quad (2.3)$$

2.2.4 Conjugate Gradient Algorithm

The Conjugate Gradient (CG) can be applied to adjust the weights of an antenna array [GiMC01]. The CG algorithm has been well defined and described in the recent years as an alternative to the widely used LMS and RLS. With the argument of not requiring matrix inversions and avoiding stability problems, the Conjugate Directions type of algorithms, such as the CG, have been conceived for solving linear systems, [HeBK99], [Goda97].

The method in general is useful for solving the following linear system:

$$\mathbf{R}\mathbf{w} = \mathbf{b} \quad (2.4)$$

In case of antenna array processing, the weights vector, \mathbf{w} , needs to be calculated, \mathbf{b} is a vector composed by N_s following desired responses, $\mathbf{R}=\mathbf{U}$ is a matrix whose M columns refer to each of the M antenna array elements and each line corresponds to each sampling period, out of the total N_s sampling periods, [ChKi92], [Goda97]. If the received signal at the antenna array is composed by $u_{n,m} = u_m(n)$ elements, matrix \mathbf{U} is as indicated below:

$$\mathbf{U} = \begin{bmatrix} u_{1,1} & u_{2,1} & \cdots & u_{1,M} \\ u_{1,2} & u_{2,2} & \cdots & \vdots \\ \vdots & \vdots & \ddots & \vdots \\ u_{N_s,1} & u_{N_s,2} & \cdots & u_{N_s,M} \end{bmatrix}. \quad (2.5)$$

Vector \mathbf{w} is composed by M elements, corresponding to each array antenna element. Since, most probably, $N_s \neq M$, an exact solution may not exist, [ChKi92].

Two types of implementation of the CG algorithm exist, depending on the data acquisition method used: sample-by-sample and block processing. For sample-by-sample processing, it is important to periodically reset the direction vector to the true gradient in

order to ensure the convergence of the algorithm. Besides sample-by-sample processing, the block-by-block method also exists. Block-by-block CG implementation requires that both \mathbf{R} and \mathbf{b} be firstly calculated. The computational complexity of this implementation depends on K ($K \leq N$), the number of iterations. For large N the computational complexity of the algorithm is K times of the complexity of the sample-by-sample CG algorithm [Bagh99].

2.3 Antenna Arrays

Usually, the radiation pattern of a single element is relatively wide, higher gains only being achieved by increasing the electric size of the antenna. In many type of communication, antennas with very high directivity are often required. Another way to increase the electrical size of an antenna is to construct it as an assembly of radiating elements in a proper electrical and geometrical configuration *antenna array*. Usually the array elements are identical; this is not necessary, but it is more practical, simple and convenient for design and fabrication, and the individual elements may be of any type (wire dipoles or loops, apertures, etc.). That constitutes a Uniform Array. The radiating characteristics of an array can be electrically controlled by the amplitude and relative phase of each individual element’s feeding current, providing means for the deployment of adaptive antennas algorithms.

The simplest kind of array is the linear one, the Uniform Linear Array (ULA), where radiating elements are placed along a line, uniformly separated in space by a constant distance d_e , as shown in Figure 2.12, and is applied for simulations for MTs.

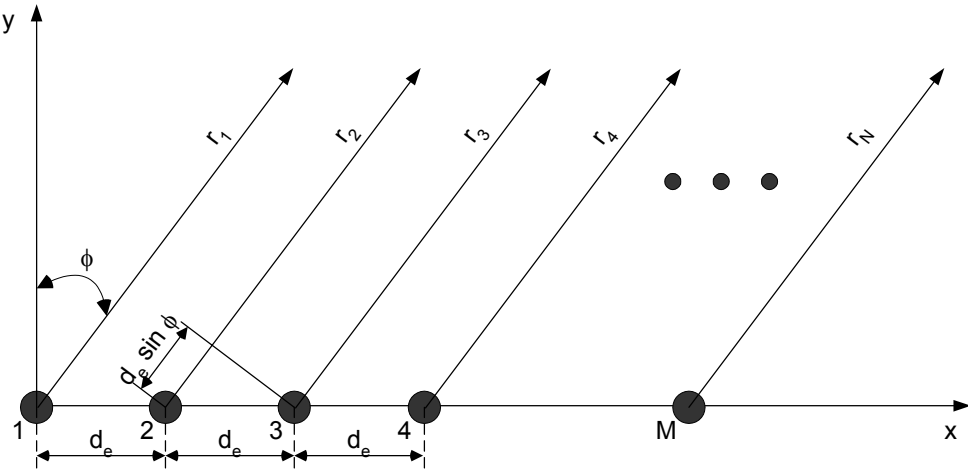


Figure 2.12 – Far-field geometry of M-element linear array of isotropic sources (extracted from [Szym02]).

An array of identical elements, all of identical magnitude, and each with a progressive phase, is referred to as a uniform array. The Array Factor (AF) of an M -element ULA of isotropic sources is given by:

$$AF = \sum_{n=1}^M e^{j(n-1)\psi} \quad (2.6)$$

where $\psi = kd \sin \phi + \gamma$, or yet as a closed form, which is more convenient for pattern analysis

$$AF = e^{j\left(\frac{M-1}{2}\right)\psi} \cdot \frac{\sin\left(\frac{M}{2}\psi\right)}{\sin\left(\frac{\psi}{2}\right)} \quad (2.7)$$

The maximum value of the magnitude of the AF is equal to M . To normalise the array factor so that the maximum value is equal to unity, the AF is written in normalised form as

$$|AF|_n = \frac{1}{M} \left[\frac{\sin\left(\frac{M}{2}\psi\right)}{\sin\left(\frac{\psi}{2}\right)} \right] \quad (2.8)$$

In the case of adaptive beamforming, ULA elements can be fed with different magnitudes and phases respectively to the weights vector provided by adaptive processor. If the elements are of any other than isotropic pattern, the total field pattern can be obtained by simply multiplying the AF by the normalised field pattern of the individual element [Bala97].

Another usual way of assembling elements consists of a circular array where a set of M elements is distributed over a circular ring, as depicted in Figure 2.13, which is referred to as Uniform Circular Array (UCA), and is applied for simulations for BS.

For an array of M isotropic elements, equally spaced on the x-y plane along a circular ring of radius r_a , the AF is given by:

$$AF(\theta, \phi) = \sum_{n=1}^M e^{jkr_a [\sin \theta \cos(\phi - \phi_n) - \sin \theta_0 \cos(\phi_0 - \phi_n)]} \quad (2.9)$$

It is worth to mention that the main ULA characteristic is its symmetry, i.e., the radiation pattern is the same to the front of the array and to the rear, while in UCA there is no such symmetry, so the beam is pointed to the specific direction. These two types of antenna arrays are presented, being most convenient and simple for the adaptive implementation to the Wideband Directional Channel Model (WDCM) simulations scenarios.

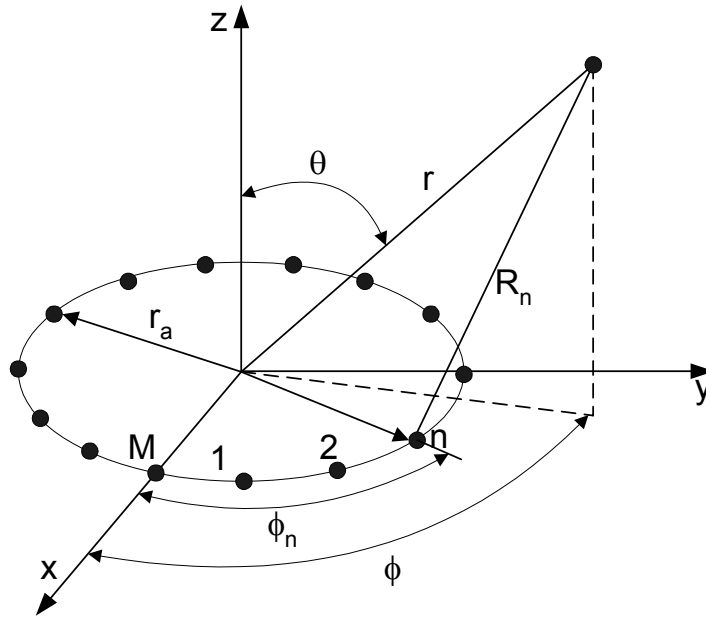


Figure 2.13 – Geometry of an M-element circular array (extracted from [Szym02]).

2.4 Wideband Propagation Channels

2.4.1 Introduction

The structure of the radio channel should be known in order to deal with beamforming and SAs. At the present, with the introduction of techniques and features that depend on the spatial distribution of the mobiles, wideband temporal and spatial information is required for relevant channel models.

Depending on the numbers of parameters used to build various channel models, one can divide them into: non-directional and directional ones. Classical, non-directional, channel models provide information on signal power level distributions and Doppler shifts of the received signal. Fundamental principles of the classical channel models are used to describe other spatial models. Early channel models accounted only for the time-varying amplitude and phase of channel. Recent, directional, channel models include both spatial and temporal features for design of wideband models; these spatial channel models build upon the classical understanding of multipath fading and Doppler spread, by incorporating additional concepts such as time delay spread, Angle-Of-Arrival (AoA), and adaptive array antenna geometries [LiRa99].

In a wireless system, a signal transmitted through the channel interacts with the environment in a very complex way. There are reflections from large objects, diffraction of

the electromagnetic waves around objects, and signal scattering. The result of these complex interactions is the presence of many signal components, or multipath signals, at the receiver.

Several directional channel models are described in detail in [LiRa99]. In the subsequent part of this section only WDCMs, based on Geometrically Based Single Bounce (GBSB) Models, are introduced.

2.4.2 Geometrically Based Single Bounce Models

Geometrically Based Single Bounce (GBSB) Statistical Channel Models are developed by defining a spatial scatterer density function [LiRa99]. From the spatial scatterer density function, it is possible to derive the joint and marginal Time-of-Arrival (ToA) and Direction-of-Arrival (DoA) probability density functions (PDF). Knowledge of these statistics is useful for evaluating adaptive antenna performance. The PDF delimiting region is discussed in what follows, leading to two different models, which are based on a scatterer region of circular and elliptical shapes, the GBSB Circular Model (GBSBCM) and GBSB Elliptical Model (GBSBEM).

The GBSBCM is applicable to macro-cell environments. In a macro-cell environment, the BS is typically deployed above the surrounding scatterers, i.e., antenna heights are relatively high, therefore assuming that there will be no signal scattering from locations near the BS. Figure 2.14 shows a circular scatterer region of radius r_{max} surrounding the MT.

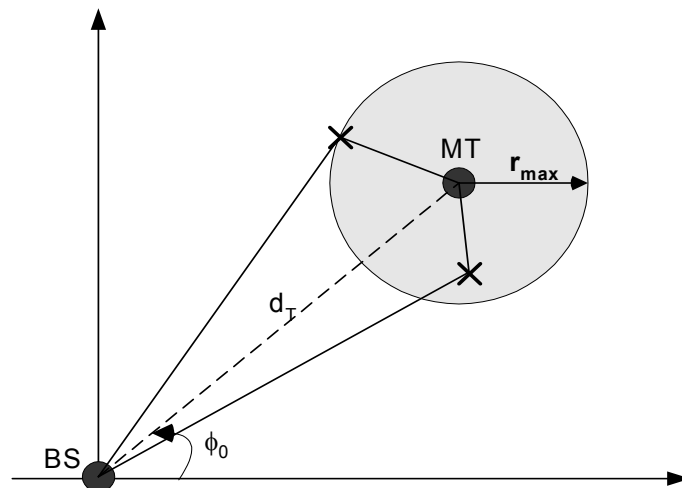


Figure 2.14 – Geometry for the GBSBCM scattering region (extracted from [ZoMa00]).

The GBSBEM is applicable to micro-cell environments, where the BS antenna heights are low, below rooftop level, and scatterers are distributed between and around both the BS and MT. Scatterers are uniformly distributed within an ellipse, as shown in Figure 2.15, where BS and the MT are at its foci.

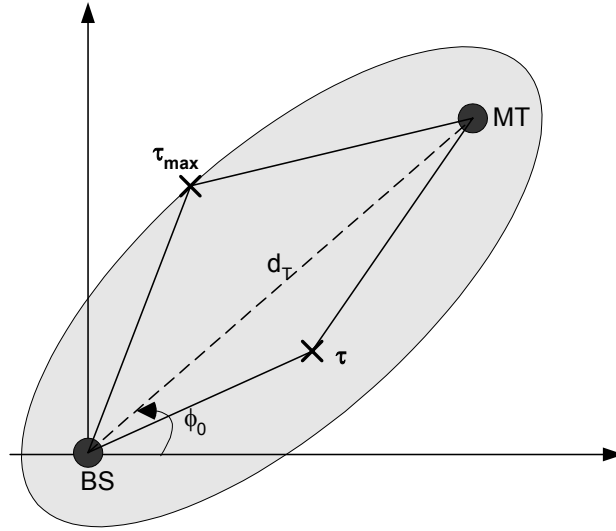


Figure 2.15 – Geometry for the GBSBEM scattering region (extracted from [ZoMa00]).

The GBSBCM joint ToA (τ) and DoA (ϕ) PDF, for both BS and MT, are [LiRa99]:

$$p_{\tau,\phi}(\tau,\phi) = \frac{(d_T^2 - \tau^2 c^2)(d_T^2 c + \tau^2 c^3 - 2\tau c^2 d_T \cos(\phi - \phi_0))}{4\pi r_{max}^2 (d_T \cos(\phi - \phi_0) - \tau c)^3} \quad (2.10)$$

where:

- c - speed of light,
- d_T – distance between MT and BS,
- ϕ – horizontal angle,
- ϕ_0 – MT angular position, defined in Figure 2.14,
- r_{max} – radius of scatterers region,
- τ – time delay (ToA)

The validity regions for the BS and MT cases are, respectively:

$$\frac{(d_T^2 - \tau^2 c^2)(d_T^2 c + \tau^2 c^3 - 2\tau c^2 d_T \cos(\phi - \phi_0))}{\tau c - d_T \cos(\phi - \phi_0)} \leq 2r_{max} \quad (2.11)$$

$$\frac{d_T^2 - \tau^2 c^2}{d_T \cos(\phi - \phi_0) - \tau c} \leq 2r_{max} \quad (2.12)$$

Out of these regions, the PDF's value is zero, which means that there are no scatterers.

For the GBSBEM, the joint PDF observed at the BS (or MT) is given by [LiRa99]:

$$p_{\tau,\phi}(\tau,\phi) = \begin{cases} \frac{(d_T^2 - \tau^2 c^2)(d_T^2 c + \tau^2 c^3 - 2\tau c^2 d_T \cos(\phi - \phi_0))}{\pi \tau_{max} c \sqrt{\tau_{max}^2 c^2 - d_T^2} (d_T \cos(\phi - \phi_0) - \tau c)^3}, & \frac{d_T}{c} \leq \tau \leq \tau_{max} \\ 0 & , \text{elsewhere} \end{cases} \quad (2.13)$$

Note that the above PDF is independent of the scattering/clustering density, for it assumes a continuous scattering distribution. However, in a simulation case, cluster density should be a parameter to take into account [ZoMa00].

2.4.3 Wideband Directional Channel Models

The used Wideband Directional Channel Model (WDCM) is based on the GBSBEM and GBSBCM, e.g., [MaCo01], for Micro-Cells (MiCs) and Macro-Cells (MaCs), respectively. Their nature is semi-statistical and geometrical, being constituted by a set of clusters of scatterers, on a horizontal plane, uniformly distributed inside elliptical or circular areas, defined by the MT or BS positions, respectively for MiCs and MaCs, [GiCo03], Figure 2.16.

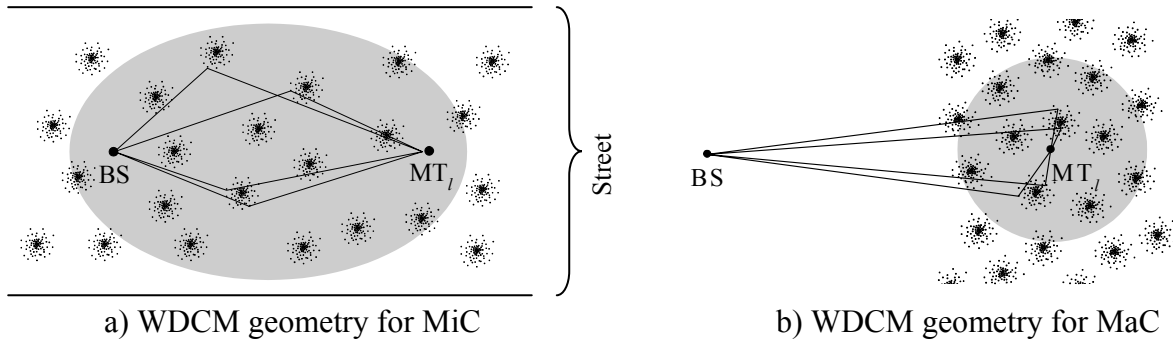


Figure 2.16 – Cluster and scatterer distributions, indicating some single-bounce reflections (extracted from [GiCo03]).

The MiC WDCM is based on the GBSBEM, assuming a Line-of-Sight (LoS) street environment. Scatterers are fixed in space and grouped into clusters, which are uniformly distributed within an elliptical scattering region. The elliptical region is limited to the street width, and both the BS and the MT are aligned with the street's axis. The location of scatterers within each cluster follows a Gaussian distribution around each cluster centre,

Figure 2.16a. Scattering coefficients are random variables, assumed uniformly distributed in amplitude and phase within $[0, 1]$ and $[0, 2\pi[$, respectively.

Besides the scenario perspective for MiC, the MaC WDCM, based on the GBSBCM, also follows the same philosophy, Figure 2.16b. The main difference is that the scattering region is a circular one, being centred at the MT. Also, the MaC model is not applicable to the street width.

That two presented models for MiC and MaC are chosen for simulations, because of their simplicity. They are based on the GBSB models, adding the characteristic feature of being statistical to better approximate the enormous variety of channel conditions.

The Modified GBSB (MGBSB) Models were created for simulation purposes [Marq01], taking into consideration the temporal evolution of the channel due to motion. It should be mentioned that the MGBSB Models used for this work, derived on IST-FLOWS (Flexible Convergence of Wireless Standard and Services) proposals [DGVC03]. The number of clusters per model usually is not more than 10 and, for simulation, 7 clusters per model are enough.

3 Implementation

3.1 General Concept of Performing the Simulation

This chapter is concentrated in the description of the models and algorithms implemented for macro- and micro-cell scenarios. The chosen scenarios introduce one MT and one BS. For that, the main parameters of the channel and general concept of performing the simulations will be firstly described.

The problem presented in this work deals with the implementation of beamforming at both the BS and the MT in the UMTS - TDD mode, and its analysis, regarding the physical wideband and directional characteristics of the channel. The analysis will be based on creating and comparing the chosen scenarios. A beamforming algorithm will control the adaptive arrays at both the BS and the MT ends, in order to minimise co-channel interference, within the same cell.

At first, the main input and output parameters of the channel should be defined. For the channel models simulation, environment type (MiC or MaC), the MT-BS distance, MT and BS antenna array parameters and scattering region also need to be defined. The other parameters concerning scatterer and cluster specific properties are listed below, [Szym02]:

- region limitation (τ_{max} or r_{max})
- cluster distribution – uniform within the scattering region
- cluster characteristics
 - distribution of scatterers within the clusters – Gaussian
 - cluster density
 - number of scatterers in each cluster – determined by a Poisson distribution
 - average number of scatterers in each cluster
- scatterer characteristics
 - scattering coefficient amplitude distribution – uniform, within [0,1]
 - scattering coefficient phase distribution – uniform, within [0,2 π [
- path attenuation coefficient
- presence or absence of LoS in the MaC case

All of these parameters are used for channel simulation, having been previously defined according to two model assessments in IST-ASILUM (Advanced Signal Processing Schemes for Link Capacity Increase in UMTS), [Hera00] and IST-FLOWS, [DGVC03]. For simulation purposes, the parameters of the channel have been chosen according to IST-FLOWS,

[DGVC03]. Some of these parameters are scenario specific, and some are scenario independent and common for all. Clusters distribution is uniform within the scattering region, and cluster density has been set to $5 \cdot 10^{-5} \text{ m}^{-2}$. The distribution of scatterers within clusters is Gaussian, with average number of scatterers per cluster of 20. Relative delays are considered as integer multiples of the chip duration, $0.26 \mu\text{s}$, for a chip rate of 3.84 Mchip/s, and all incoming signals are assumed to arrive at the same instant of time, only allowing for inter-cluster delays, [GiCo02].

For simulation, the IST/TUL Wideband Double Directional Channel Model (IST/TUL – WDDCM) simulation software will be applied. The simulation software generates the magnitudes (or power), delay (or ToA), phase, AoA and AoD of each scattered ray as outputs from a simulation concretisation, or from a programmed sequence of concretisations. The output parameters of the channel, obtained from the WDDCM and referred to the Directional Channel Impulse Responses (DCIRs) are the main input parameter for the present implementation. A DCIR provides the information on AoA, AoD, ToA, magnitude (or power) and phase of incoming signal, which are required from the wideband system perspective and also to take into account the directional requirements of beamforming. The angular resolution of WDDCM used in simulations has been set to 0.5° , [Gil04].

In Figure 3.1, a flowchart presents the general concept of performing the beamforming simulations that have been conceived in [Gil04], for a single link, single beamformer (at either BS or MT).

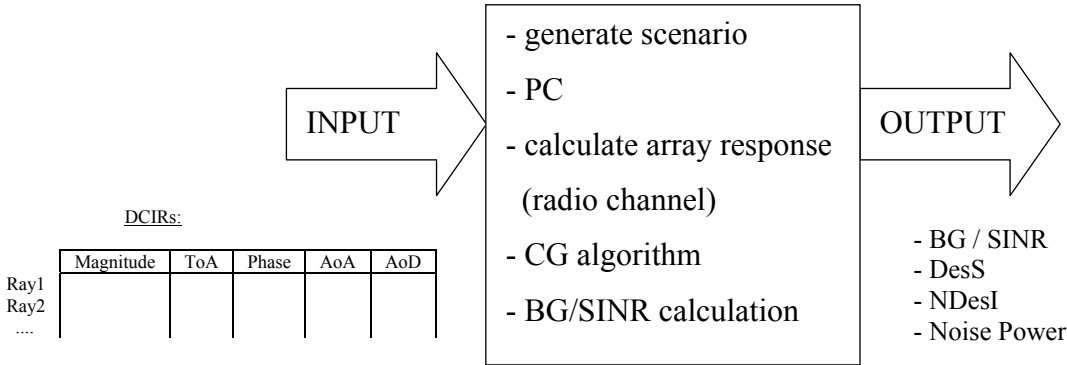


Figure 3.1 – General concept of performing each beamforming simulations.

The simulator gives a regular text file with 5 columns, for each DCIR, and each of the columns corresponds to different parameters associated to each ray. The first column, in this file, is magnitude, then ToA, phase, AoA, and AoD respectively.

It should be mentioned that the general block of Figure 3.1, considers:

- Generation of chosen scenarios
- Implementation of PC
- Calculation of array response (radio channel)
- Implementation of CG algorithm
- BG / SINR calculation.

Generation of chosen scenarios will be followed with the description given by separate parts, Section 3.2, whereas the rest of these several elements of the simulation flowchart will be described below.

A PC mechanism has been applied, using MATLAB® (file `power_control.m`). A simple but effective PC process is implemented, in order to avoid near-far effects. The PC algorithm, which has been applied for simulations, is described in [Gil04].

The next step to perform the beamforming simulations, the calculation of array responses, depends on the number of L active BS-MT links and the number of antenna elements, M . For each array element, for all active BS-MT links and for each time and angle sample of the DCIR, each element of array responses is a product of:

- combination of channelisation and scrambling codes, which characterises each active BS-MT pair
- DCIR magnitude
- DCIR phase
- antenna Array Factor (amplitude + phase)

As a result of this multiplication, channel matrices are obtained for all L active links. These results are added with antenna thermal noise, N , creating a single array response matrix [Gil04].

Making use of previous work, [Szym02], the CG algorithm has been applied as an internal function (`pcg.m`), to control the beamforming process, by choosing the weights vector. This is consistent with the description provided in Section 2.2.4.

As it is shown in Figure 3.1, as an output, the objective is to calculate the BG and SINR for a single antenna's element and for each link, as it was described in Section 2.2.3. For all simulations, only SINR and BG values from the number of iteration

obtained for maximum SINR will be taken into account. The average value of SINR and BG is obtained from 300 concretisations, as well as the standard deviation, giving a view on the whole distribution of values, and to ensure that the number of concretisation is sufficient. Besides evaluating SINR and BG, it is important to mention other outputs, which could be analysed, the Desired Signal (DesS), Non-Desired Interference (NDesI) and noise power components.

To obtain the reference source for the non-blind adaptive algorithm implementation, TDD channelisation and scrambling code sequences combination are generated. The codes have been applied, using MATLAB®, and built according to the code tree, as it is shown in Figure 2.6. The code length is constant and equal to 16, and SF is set to 4.

Simulations are performed using linear and circular arrays with different number of elements, 8 for ULA, with element spacing of $\lambda/2$, oriented with its normal in the direction considered as 0° , which is coincident with the LoS direction, on the same horizontal plane as the WDCM, and 12 for UCA with element spacing of $3/4 \lambda$. The 180° sectorisation has been considered for ULA case, assuming also that antenna array has a ground backplane, ideally not receiving any signals from behind. This concept has been chosen according to [Szym02].

The general structure and some components of the simulations, for this work, have been derived on the basis of work made for UMTS - FDD mode, with an adaptive array at the BS, [Szym02], [Olej02], with the following changes for the UMTS - TDD mode application:

- scrambling sequences and channelisation codes for TDD mode have been added to substitute the FDD codes,
- filtering of DCIRs needs to be apply to get the ToA per each chip duration, and AoD that are need in case of dealing with the beamforming at the both side,
- moreover, the whole structure of the program has been changed to obtain as main target, beamforming at both the BS and the MT.

The general steps of performing each beamforming simulations, to obtain beamforming at both the BS and the MT, are shown in Figure 3.2. The first step depicts a beamforming only at the BS, i.e., the MT transmitting to the BS with a single, omnidirectional antenna and beamformer is generated at the BS. The two other steps depict the main concept of this study, beamforming at the both the BS and the MT. At the second

step, a beamformer is generated at the MT, whereas at third step a beamformer is generated at the BS.

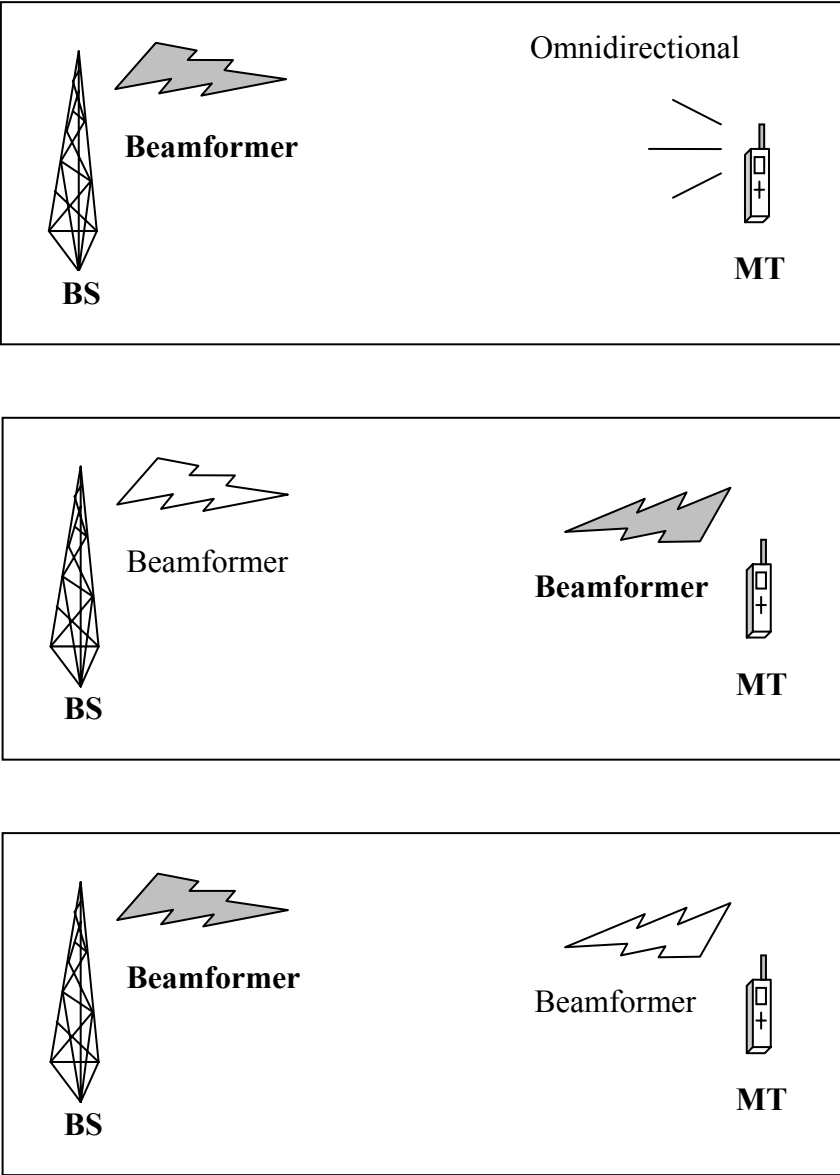


Figure 3.2 - General steps of performing each beamforming simulations.

Additional to Figure 3.1 and Figure 3.2, which present the general concept and steps of performing the simulations, a simulation flowchart, Figure 3.3, goes into detail of the whole structure of the simulations that have been implemented for this study.

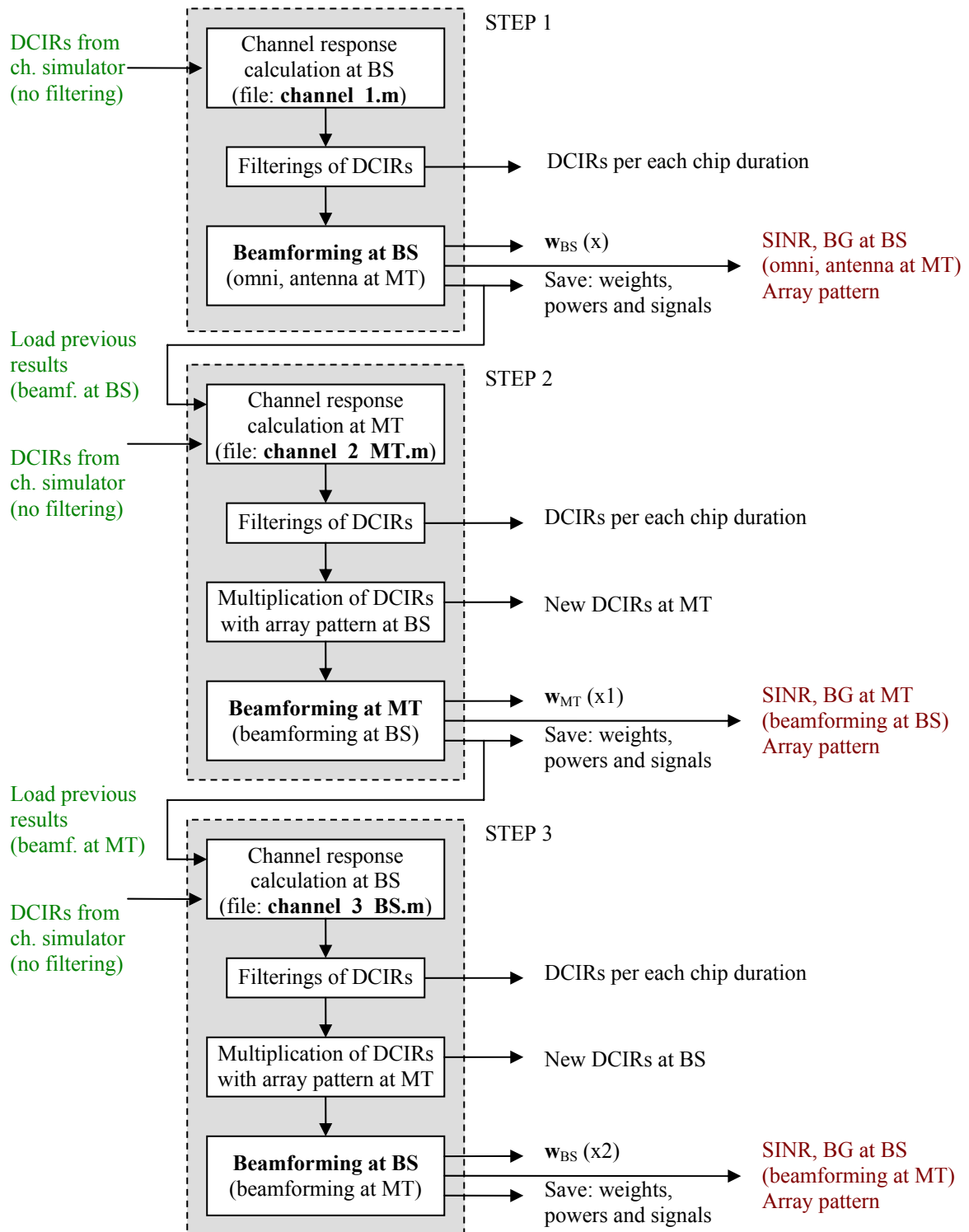


Figure 3.3 – Simulation flowchart.

As it was already mentioned, the simulations have been performed to obtain beamforming at both the BS and the MT. The whole structure of performing the simulation is divided into three programs:

- file *channel_1.m*, (beamforming at the BS and single antenna at MT),
- file *channel_2_MT.m*, (beamforming at MT with beamforming at the BS),
- file *channel_3_BS.m*, (beamforming at the BS with beamforming at MT).

The first part of the simulation (file: *channel_1.m*) deals with beamforming at the BS and a single omnidirectional antenna at the MT. To obtain the array pattern, SINR and BG at the BS, the general concept of performing the simulation, Figure 3.1, is used. Having the beamforming at the BS, the second part of simulation (file: *channel_2_MT.m*) is applied for obtaining the beamforming at the MT. Firstly, previous results (weights, power and signals) from the first part of simulations, and DCIRs from channel simulator are loaded. Having new inputs, filtering of DCIRs needs to be apply to get the ToA, per each chip duration, and AoD, which are need in case of dealing with the beamforming at the both side. At first the DCIRs are divided in bins, with a chip duration of $0.26 \mu\text{s}$, then one signal (amplitude and phase) is calculated per bin, being the sum of the all signals inside the bin. Moreover to calculate the ToA and angles (AoA, AoD), a weighted mean of all ToA and angles per bin is calculated. The results after filtering, new DCIRs, are multiplied by an amplitude and phase given by the BS array pattern, for each AoD (AoAs at the BS in the UL will be the AoDs at the BS in the DL). It was verified, by making the test calculations in MATLAB®, that filtering and multiplication works properly. Moreover, after filtering and multiplication, all further calculations follow the description provided in Figure 3.1. Finally the results from the second part of the simulation are loaded into the last part (file: *channel_3_BS.m*), to calculate the beamforming at the BS, with array pattern at MT.

The outputs of the simulations provide several values and parameters, which are further used for a variety of analysis, comparisons and conclusions. All calculations have been implemented using several files in MATLAB®.

3.2 Multi-user Scenarios

The scenarios that have been defined for MiC, MaC and “*hybrid*” MiC-MaC environments aim to depict practical situations, concerning the angular positions of MTs, their distance from BS and number of users. The MiC scenarios depict situations applied to

urban settings, for UMTS, whereas MaC and “*hybrid*” MiC-MaC scenarios depict situations applied to sub-urban or rural environments, where the covering BS antenna will be much higher than the MTs, being able to cover larger BS-MT distances.

The MiC scenarios that have been proposed for simulation, Table 3.1, present streets and plaza scenarios. The streets examples have been divided into three groups: the first one, Sc#MiC_a, depicts one BS and one MT, being placed at the same LoS from the BS. The distance between the BS and the MT is set to 200, 500 and 1000 m, to verify the dependence of beamforming performance on BS-MT distance; the other two streets scenarios, Sc#MiC_b, Sc#MiC_c, depict two MTs, being placed at the same LoS from the BS and assume constant BS-MT distance of 500 m, whereas between MT₁ and MT₂ distance is set to 50 or 500 m. These two scenarios also depict different transmissions, where in Sc#MiC_b, MT₁ is in UL, besides MT₂ being in DL transmission, whereas Sc#MiC_c depict opposite transmissions, i.e. MT₁ is in DL and MT₂ is in UL. Finally, the last scenario from Table 3.1, Sc#MiC_d, has been proposed to show the angular positions of MTs. This scenario presents two MTs at the same 100 m distance from BS, and the same 50 m distance between MTs, being placed at a plaza 15000 m².

The MaC scenarios, presented in Table 3.2, have been proposed to compare the beamforming performance between MiC and MaC environments. These scenarios are similar to the MiC scenarios, Table 3.1, but they cover larger BS-MT distances. The first scenario, Sc#MaC_a, proposed for this study, depicts one BS and one MT, being placed at the same LoS from the BS, similar to Sc#MiC_a, but with larger BS-MT distances, being set to 1000, 1500 and 2000 m. The other two “*hybrid*” scenarios, Sc#H_MiC-MaC_a, Sc#H_MiC-MaC_b, present two MTs, being considered as MiC on the street, placed at the same LoS and at the same 1000 m distance from the BS, but with different distance between each MT, i.e., distance between MT₁ and MT₂ is set to 50 or 500 m. These scenarios also depict different transmissions; in Sc#H_MiC-MaC_a, MT₁ is in UL and MT₂ is in DL, whereas Sc#H_MiC-MaC_b depicts opposite transmission, i.e., MT₁ is in DL and MT₂ is in UL. Finally, Sc#H_MiC-MaC_c has been identified to verify the dependence of beamforming performance on angular positioning of MTs. This scenario assumes constant BS-MT distance, being set to 1000 m, but different positions from the BS. The distance between MT₁ and MT₂ is set to 50 or 500 m.

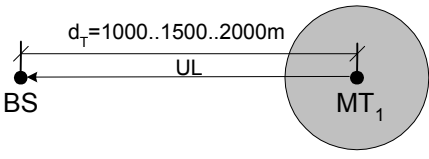
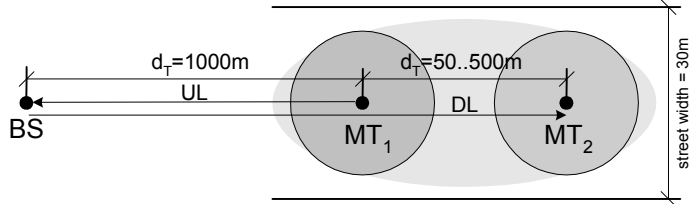
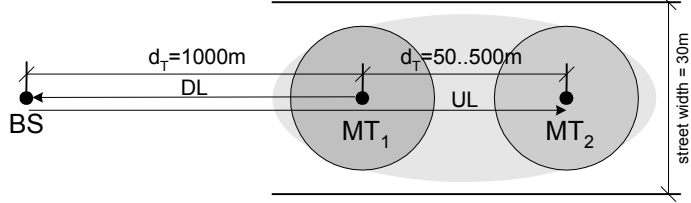
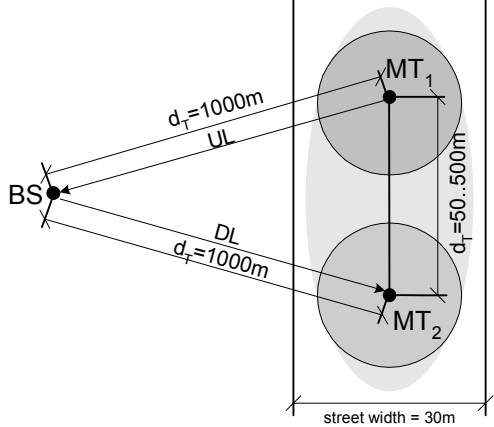
The MiC and MaC scenarios that have been chosen for simulation, for this work, Sc#MiC_a and Sc#MaC_a, can verify the dependence of beamforming performance

on BS-MT distance, whereas dependence on number of user and angular positions of MTs are not considered in this work.

Table 3.1 – WDCM micro-cell scenarios.

| Sc # | Scenario (not to scale): |
|-------|--------------------------|
| MiC_a | |
| MiC_b | |
| MiC_c | |
| MiC_d | |

Table 3.2 – WDCM macro-cell scenarios.

| Sc # | Scenario (not to scale): |
|-------------|--|
| MaC_a |  |
| H_MiC-MaC_a |  |
| H_MiC-MaC_b |  |
| H_MiC-MaC_c |  |

4 Analysis of Results

4.1 Initial Considerations

This chapter deals with analysis and simulation results obtained from simulations made according to the chosen scenarios. Generally, these analyses are made for MaC and MiC environments, and are divided into two groups. The first group consists of the analysis of simulations obtained for MaC, and the second one obtained for MiC. At first, some initial consideration are presented, then, in each scenario, Sc#MaC_a, Sc#MiC_a, for MaC and MiC respectively, results are analysed to show and describe characteristic of each chosen scenarios. Finally, a general conclusion and some array radiation patterns, obtained from simulations, are presented.

At the beginning, some general observations are presented to shown that the CG algorithm works properly. It should be noticed that the CG converges along the number of iterations. These observations are common for all chosen scenarios, and for all steps of performing the beamforming, presented in the previous chapter. Figure 4.1a and Figure 4.1b shows the behaviour of BG during CG iterations, for chosen scenarios for MaC and MiC, respectively. It is confirmed that for all simulated scenarios CG algorithm converges to the maximum value of BG at most in the $M=6^{\text{th}}$ iteration (usually started at 5^{th}), and keeps the BG value constant for higher number of iterations.

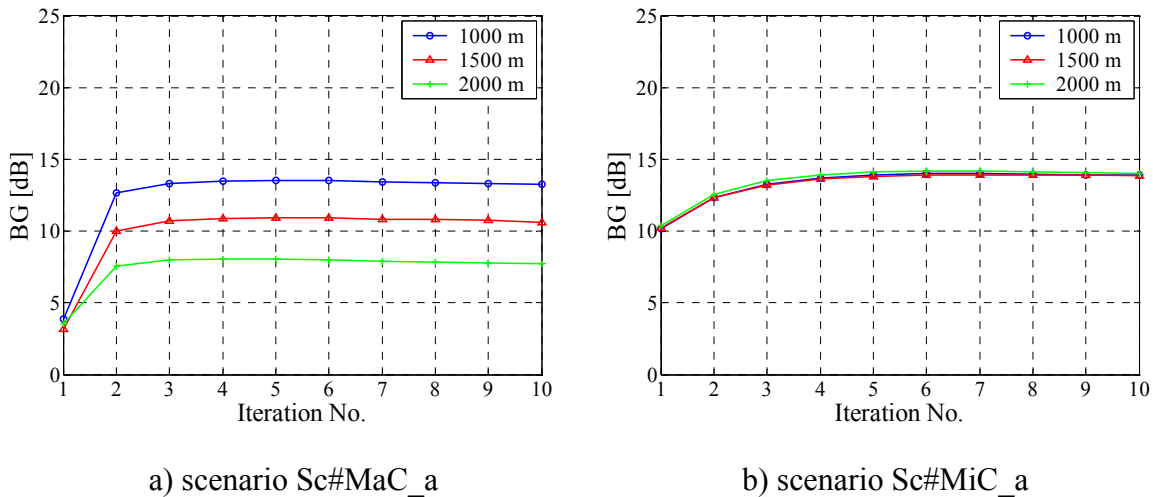
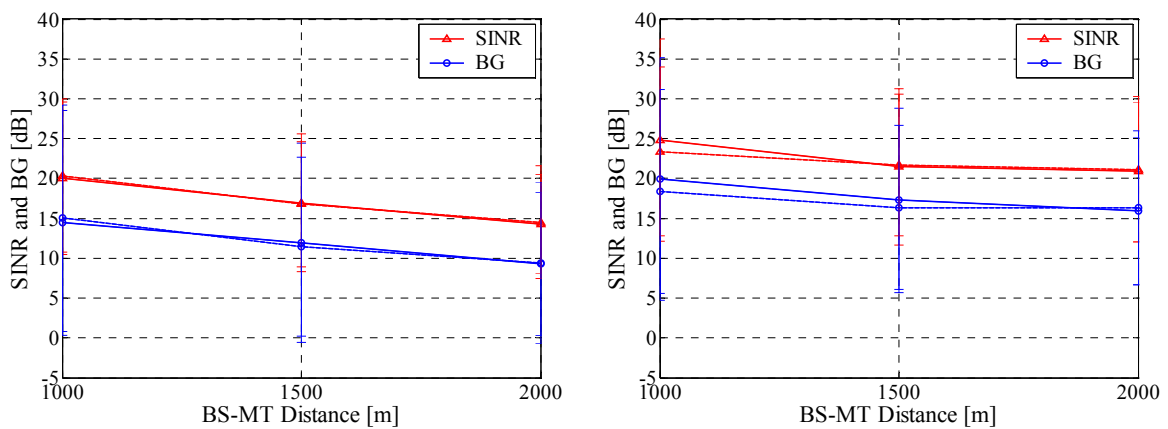


Figure 4.1 – Examples of BG evolution as a function of iteration number.

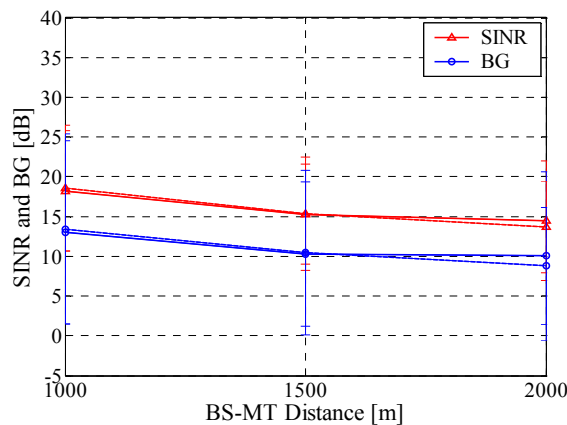
Since this behaviour is similar for all scenarios, the evaluation of BG with the number of iteration is no longer presented in this chapter. In the annexes, one can find the evaluation of BG with the number of iterations for all scenarios and for all steps of beamforming. For all analyse, only SINR and BG values from the number of iteration obtained for maximum SINR along concretisations will be taken into account.

It should be mentioned that all simulations have been done for 300 independent concretisations of DCIRs. Additionally, it has been compared to the result achieved for another, independent group of 300 channel realisations, to shown that for the same number of concretisations, results are not so different, as one can see in Figure 4.2.



a) 1st step of beamforming

b) 2nd step of beamforming



a) 3rd step of beamforming

Figure 4.2 – Comparison between two independent groups of 300 channel realisations for scenario Sc#MaC_a.

In Figure 4.2a, one can notice that the difference between BG values achieves less than 0.5 dB for 1000, 1500 and 2000 m, for the 1st step of beamforming. However, one should be aware that a difference or inaccuracy can happen for the 2nd and 3rd steps of beamforming; as one can see in Figure 4.2b, for 1000 and 1500 m, and in Figure 4.2c, for 2000 m, the difference between BG values obtained for another channel model simulation, but for the same number of 300 concretisations is around 1.5 dB.

After making this comparison, Figure 4.2, one can assume that 300 concretisations seem to be enough, and increasing the number of concretisations does not lead to increasing the accuracy of results. Moreover, simulations with 300 concretisations are already time-consuming, so increasing the number of concretisations does not seem adequate.

Also, one can observe that the mean values for each distance fit within standard deviation borders, which implies that simulations results are statistically meaningful, and precise enough.

4.2 Macro-cell Analysis

In this section, the chosen scenario, Sc#MaC_a, for MaC environments has been simulated and analysed. This scenario consists of one MT located at the same LoS from the BS with different distance between the BS and the MT, 1000, 1500 and 2000 m. This scenario has been simulated in order to show BG and SINR dependency on the different distances. Table 4.1 presents the average SINR and BG along the 300 concretisations for all steps of beamforming.

Table 4.1 – Simulation results for MaC; scenario Sc#MaC_a.

| Sc# | Step | Distance [m] | SINR [dB] | BG [dB] |
|-------|------|--------------|-----------|---------|
| MaC_a | 1 | 1000 | 20,03 | 14,43 |
| | | 1500 | 16,96 | 11,95 |
| | | 2000 | 14,32 | 9,27 |
| | 2 | 1000 | 24,85 | 19,93 |
| | | 1500 | 21,48 | 17,26 |
| | | 2000 | 20,89 | 15,92 |
| | 3 | 1000 | 18,21 | 13,02 |
| | | 1500 | 15,30 | 10,32 |
| | | 2000 | 14,46 | 10,07 |

As it is shown in Table 4.1, one can observe that the SINR and BG have a tendency to decrease when the distances increases. By analysing Table 4.1, one can notice that BG values obtained at the BS (1st and 3rd step), varying from 9.27 to 14.43 dB, whereas BG values obtained at the MT (2nd step), are larger and occur between 15.92 and 19.93 dB.

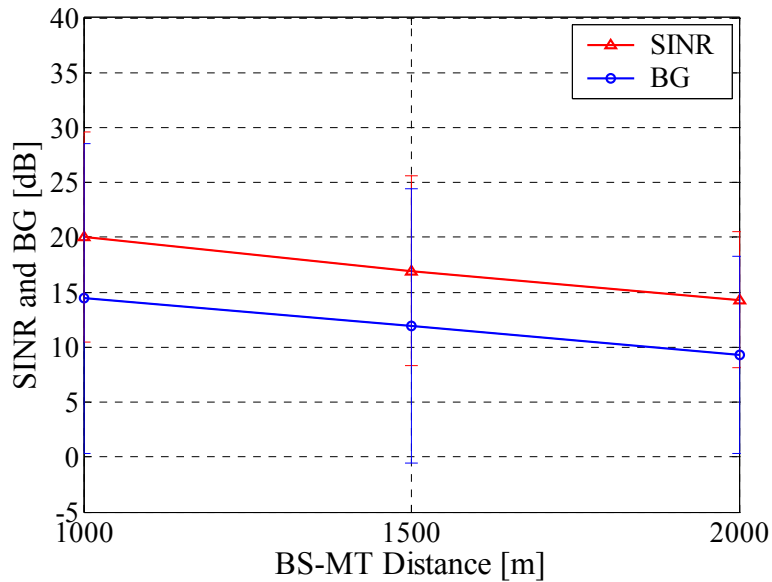


Figure 4.3 – BG and SINR as a function of BS-MT distance for the 1st step of beamforming; scenario Sc#MaC_a.

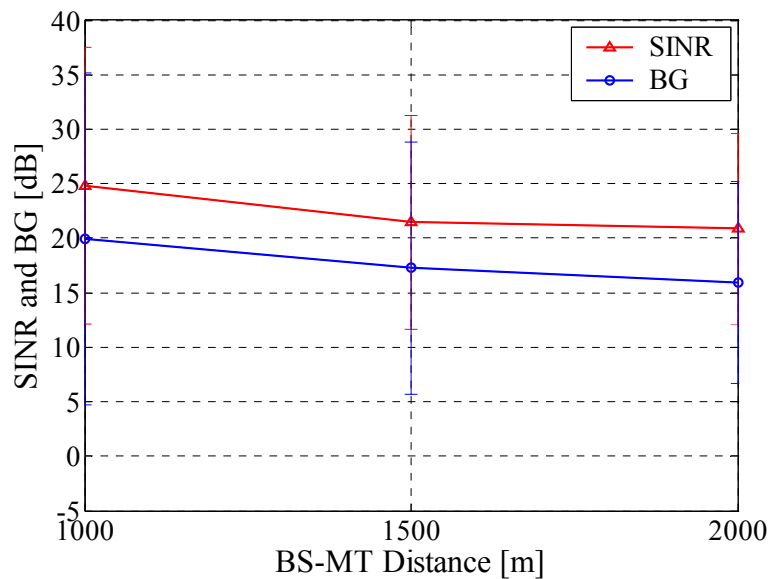


Figure 4.4 – BG and SINR as a function of BS-MT distance for the 2nd step of beamforming; scenario Sc#MaC_a.

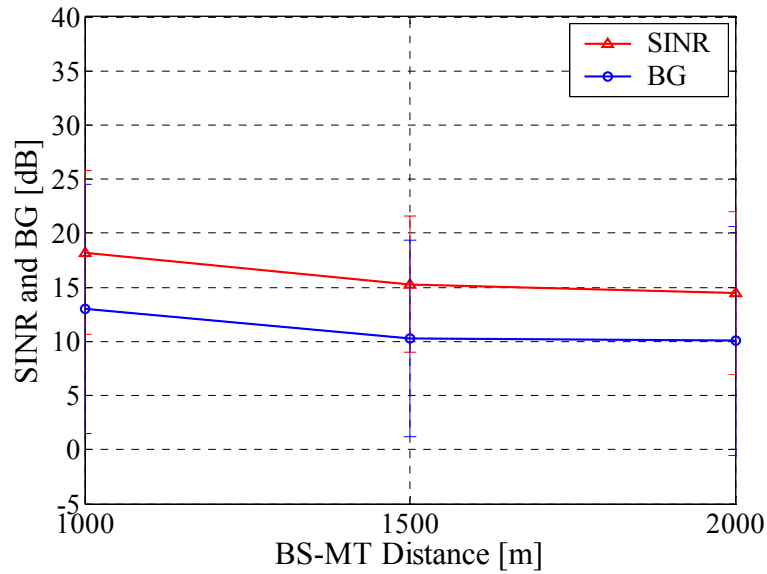
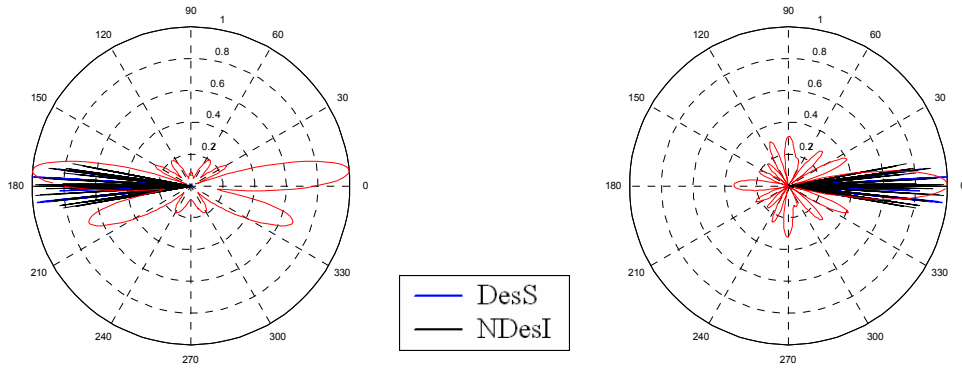


Figure 4.5 – BG and SINR as a function of BS-MT distance for the 3rd step of beamforming; scenario Sc#MaC_a.

Figure 4.3, Figure 4.4, and Figure 4.5, present BG and SINR results as a function of distances, for each step of beamforming. One can observe that the BG has a tendency to decrease with distance, which is presented also at Table 4.1, and which was verified also in [Gil04], [Szym02]. In MaCs, when the GBSBCM is applied and scatterers occur inside the circle around the MT, where the uniform linear array with 180° sectorisation prevents signals being received from behind, the BG results are larger, because signals are more widely spread all around the MT.

Finally, comparing all results from each step of beamforming, it is visible that all BG results lead to positive gain. The highest BG has been obtained for smaller distances between the BS and the MT.

Figure 4.6 presents antenna's radiation patterns, obtained for MaC, being verified that the IST/TUL-WDDCM simulation software works properly in the case of MaC. One can observe few DesS and more NDesI, which is obvious from the practical point of view, and it was also verified in [Gil04], [Olej02], [Szym02]. The radiation pattern shows, in each case, that the main beam is steered to DesS, which arrives from the BS or MT at the angle of 0°. In the annexes, one can find the antenna's radiation patterns for all scenarios, for all distances, and for all steps of beamforming.



a) ULA for 2nd step of beamforming

b) UCA for 3rd step of beamforming

Figure 4.6 – Comparison of radiation patters for ULA and UCA, for 1500m BS-MT distance; scenario Sc#MaC_a.

4.3 Micro-cell Analysis

The second part of simulations has been made for a MiC environment. The chosen scenario, Sc#MiC_a, depicts similar conditions to the MaC situation, with one MT located in LoS to the BS, but with shorter distance between the BS and the MT, 200, 500 and 1000 m. This scenario has been simulated in order to show BG and SINR dependency on the different distances in a MiC environment.

Table 4.2 – Simulation results for MiC; scenario Sc#MiC_a.

| Sc# | Step | Distance [m] | SINR [dB] | BG [dB] |
|-------|------|--------------|-----------|---------|
| MiC_a | 1 | 200 | 20,57 | 14,53 |
| | | 500 | 20,70 | 14,44 |
| | | 1000 | 20,81 | 14,74 |
| | 2 | 200 | 17,04 | 11,03 |
| | | 500 | 17,03 | 11,03 |
| | | 1000 | 17,03 | 10,89 |
| | 3 | 200 | 20,86 | 14,67 |
| | | 500 | 20,71 | 14,71 |
| | | 1000 | 20,51 | 14,80 |

As it is shown at Table 4.2, one can see that the SINR and BG achieve nearly the same constant value for different distances, oscillating only around 1 dB. For the 2nd step of beamforming, when the beamforming is generated at the MT with the beamformer at the BS, the SINR and BG values are lower than for the 1st and 3rd step of beamforming.

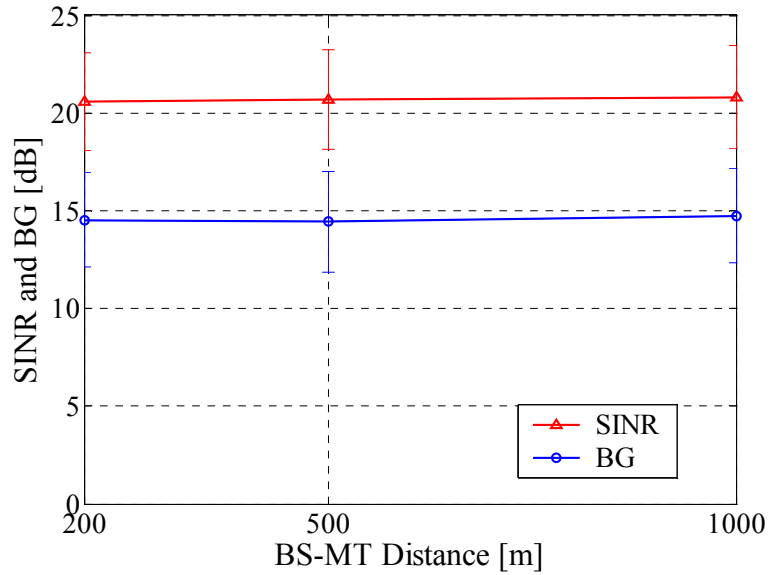


Figure 4.7 – BG and SINR as a function of BS-MT distance for the 1st step of beamforming; scenario Sc#MiC_a.

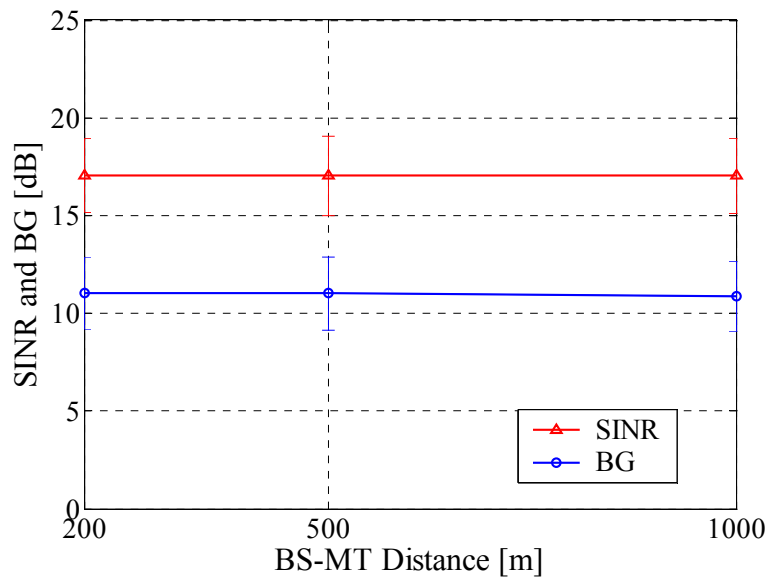


Figure 4.8 – BG and SINR as a function of BS-MT distance for the 2nd step of beamforming; scenario Sc#MiC_a.

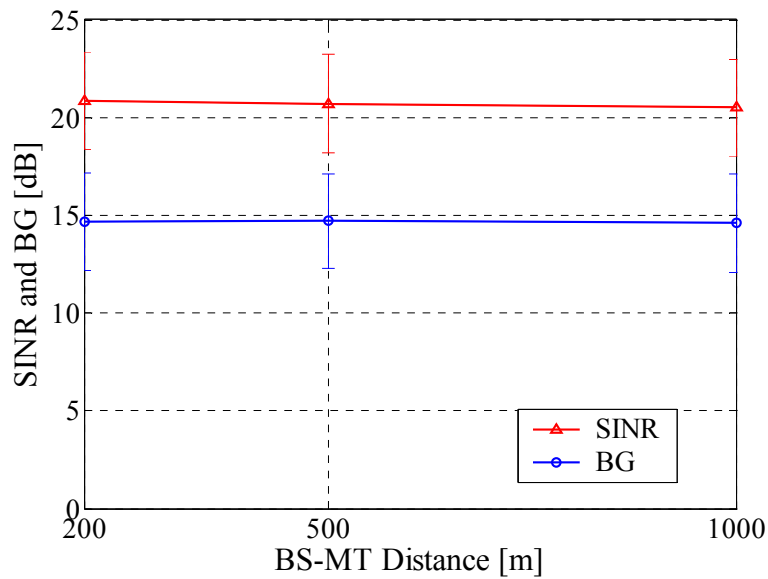
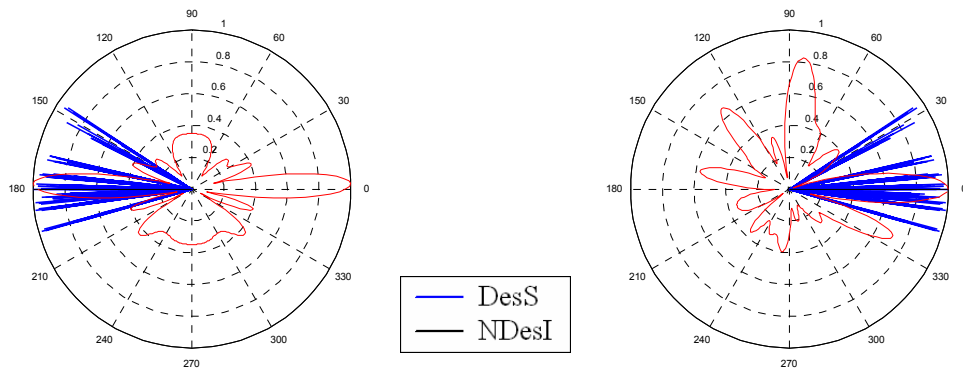


Figure 4.9 – BG and SINR as a function of BS-MT distance for the 3rd step of beamforming; scenario Sc#MiC_a.

Figure 4.7, Figure 4.8, and Figure 4.9, present BG and SINR results as a function of distance. All figures present the same constant trend for increasing distances. The BG values obtained at the MT are lower, than the ones obtained at the BS. It is expectable that the BG results are lower, because in MiC, when the GBSBEM is applied, both the BS and the MT are at the foci of ellipse, and the scatterers are around the MT, as well as around the BS, where uniform linear array with 180° sectorisation is applied, and the signals that are coming from the back are not consider at the MT array. Moreover, from the theoretical point of view, the angular spread is much lower at the MiC, DesS and NDesI are closer together in angle, which makes the DesS harder to separate from all arriving signals, [Gil04], [Olej02].

All obtained BG values for MiC are positive, but one should be aware that the results could be different, because the simulations, especially the antenna’s radiation patterns, Figure 4.10, shown that the IST/TUL–WDDCM simulation software gives a lot of DesS and only few NDesI, for MiC environment, independent on performing the beamforming simulations. It is important to mention, that the results for MiCs should be study more, and older, first version of channel model simulation software should be used in the case of MiC.



a) ULA for 2nd step of beamforming

b) UCA for 3rd step of beamforming

Figure 4.10 – Comparison of radiation patters for ULA and UCA, for 500m BS-MT distance;
scenario Sc#MiC_a.

5 Conclusions

In this thesis, Adaptive Beamforming at both the BS and the MT in the UMTS – TDD mode, in macro- and micro-cell environments has been studied. The influence in BG and SINR of the beamforming is studied, depending on a directional propagation channel model, namely in terms of the distance between mobile terminal and base station.

At the beginning of this work, the general characteristics of UMTS have been described, from UMTS architecture and to WCDMA radio interface. It also contains a brief description of the FDD and TDD modes, the two basic operations performed in the code domain (spreading and scrambling), and two important aspects in UMTS: PC and interference, focusing on TDD mode. Since UMTS is an interference limited system, interference is the major limitation in the performance of the cellular radio system. It can be reduced by sectorisation, beamforming techniques and power control. PC is essential for WCDMA cellular systems, being needed to keep the interference levels at minimum in the radio interface, and also to supply the required QoS. All of these theoretical aspects have been describe to give an overall view on all aspects that one should know, when dealing with beamforming in UMTS.

A general overview of smart antennas and adaptive algorithms is presented. The choice of an algorithm is crucial in terms of performance. The chosen algorithm, CG, has been described in detail and it has been chosen because it has the fastest convergence, good stability, and acceptable computational complexity. Also, the theory of linear and circular arrays is presented, since these two types of antenna arrays are simple and useful for analysis, being at the same time good for beamforming purposes. A linear array is easy to implement and to feed with proper currents, but it radiates power to the front as well as to the back. A circular array can steer the main beam to any direction in angular range of $[0; 2\pi[$, and it is more difficult to implement and to feed.

Wideband propagation channel models are described and for simulation purposes, the GBSBCM and GBSBEM have been applied, giving the advantage of being quite precise, like geometrical models, and quite simple, like the statistical ones.

The implementation of the adaptive algorithm and channel models is presented in detail in Chapter 3. All simulations have been performed using MATLAB[®]. The general structure and some components of the simulations have been derived on the basis of the work made for the UMTS - FDD mode, with an adaptive array at the BS, by [Szym02], [Olej02],

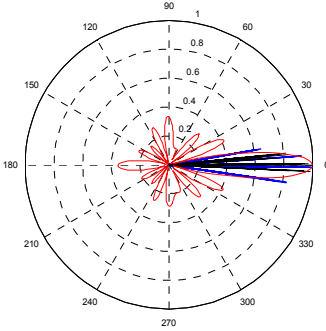
but it required changes for the TDD mode, and to include beamforming at the both the BS and the MT. Filtering of DCIRs has been added, to get the ToA per each chip duration, and AoD, which are need when one is dealing with the beamforming at the both sides. The multiplication of filtered DCIRs by amplitude and phase from the BS or MT array patterns, for each AoD, has been also added. Moreover, the whole structure of the program has been changed to perform the BS-MT beamforming all together. Finally, several scenarios are proposed, but for simulation only two have been chosen for MaC and MiC.

The analysis of performance, in Chapter 4, has been divided into two groups, MaC and MiC. In each of these groups, the chosen scenario has been analysed to show the behaviour of BG and SINR and dependency on distances between the BS and the MT. Finally, some array radiation patterns, obtained from simulations, are also presented.

Generally, after analysing the influence of beamforming one can notice that the BS-MT distance has impact for MaC scenario. The analysis also shows that for the MiC scenario, the BS-MT distance has no impact, modifying the BG only by the order of 0.5 dB. These observations show that beamforming can really have a very positive impact, but one should be aware that is not always the case.

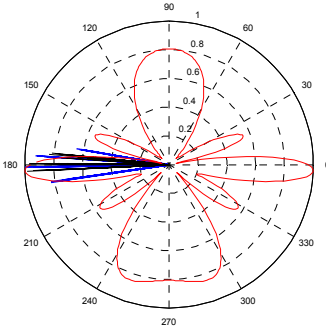
It should be noticed that in future work some more scenario should be examined. Firstly, scenarios with more users and then the “hybrid” scenario seem very interesting in terms of beamforming. It is also important to perform the MiC analysis with different channel model simulation software.

Annex A – Comparison of radiation patterns

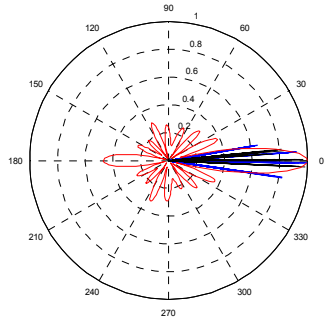


a) UCA for 1st step of beamforming

— DesS
— NDesI

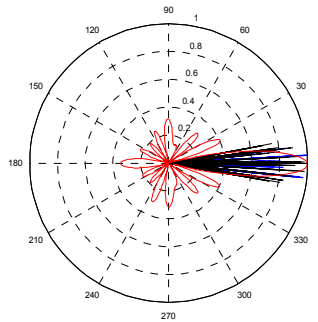


b) ULA for 2nd step of beamforming

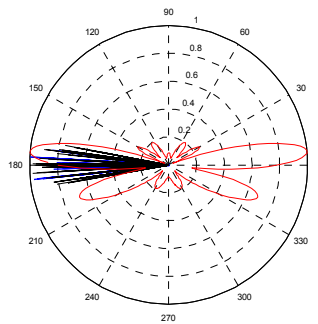
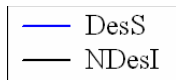


c) UCA for 3rd step of beamforming

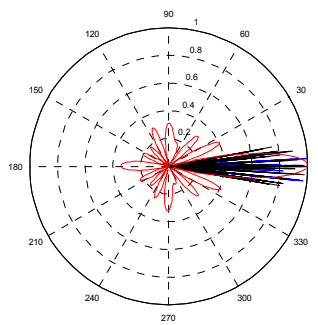
Figure A.1 – Comparison of radiation patterns for MaC, for BS-MT distance set to 1000 m; scenario Sc#MaC_a.



a) UCA for 1st step of beamforming

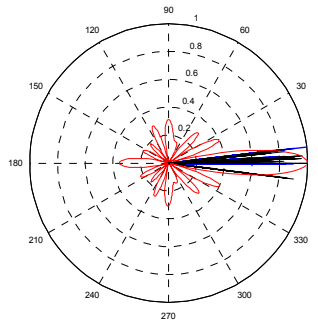


b) ULA for 2nd step of beamforming

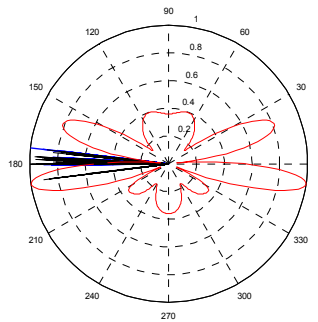
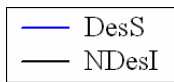


c) UCA for 3rd step of beamforming

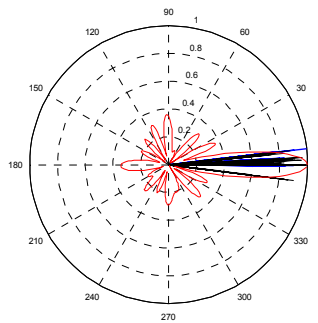
Figure A.2 – Comparison of radiation patterns for MaC, for BS-MT distance set to 1500 m;
scenario Sc#MaC_a.



a) UCA for 1st step of beamforming

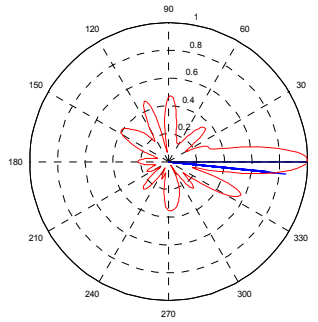


b) ULA for 2nd step of beamforming

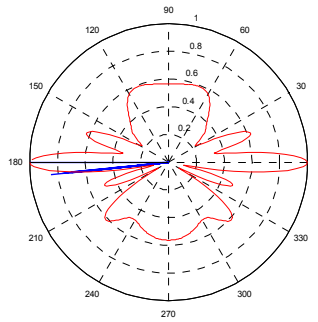
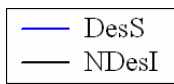


c) UCA for 3rd step of beamforming

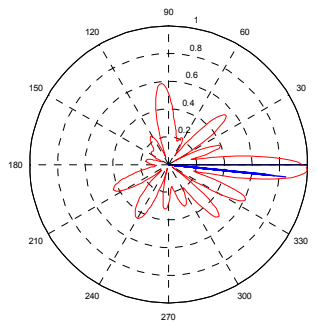
Figure A.3 – Comparison of radiation patterns for MaC, for BS-MT distance set to 2000 m;
scenario Sc#MaC_a.



a) UCA for 1st step of beamforming

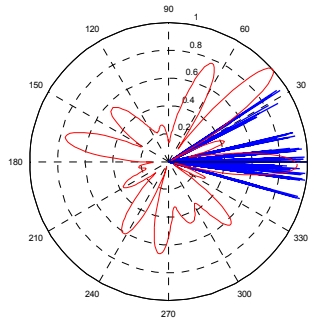


b) ULA for 2nd step of beamforming

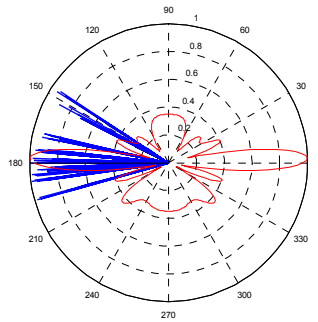
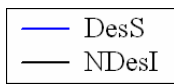


c) UCA for 3rd step of beamforming

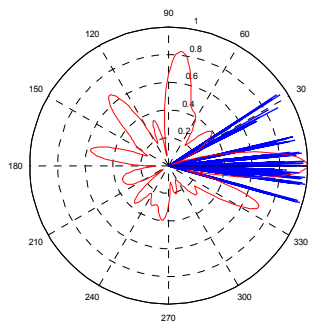
Figure A.4 – Comparison of radiation patterns for MiC, for BS-MT distance set to 200 m; scenario Sc#MiC_a.



a) UCA for 1st step of beamforming

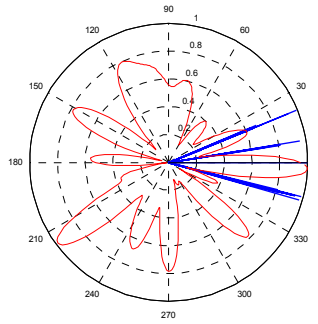


b) ULA for 2nd step of beamforming

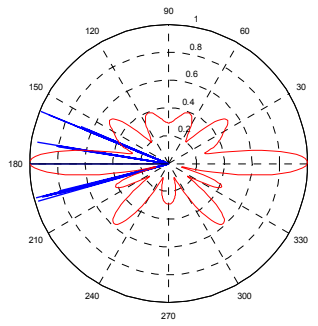
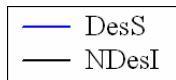


c) UCA for 3rd step of beamforming

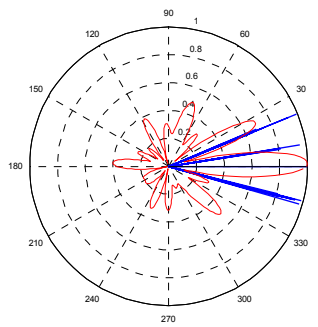
Figure A.5 – Comparison of radiation patterns for MiC, for BS-MT distance set to 500 m; scenario Sc#MiC_a.



a) UCA for 1st step of beamforming



b) ULA for 2nd step of beamforming

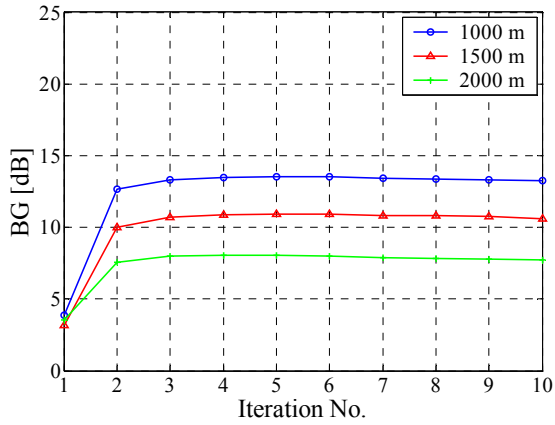


c) UCA for 3rd step of beamforming

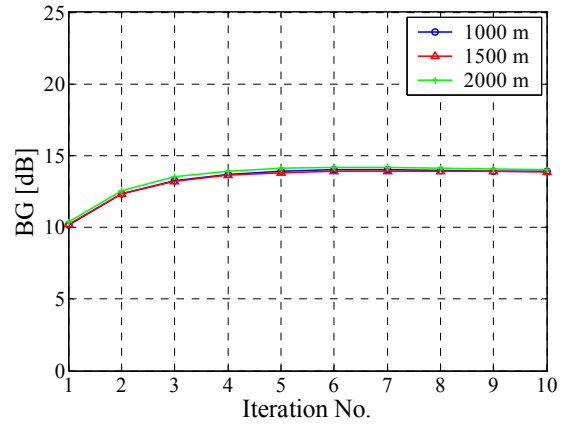
Figure A.6 – Comparison of radiation patterns for MiC, for BS-MT distance set to 1000 m;
scenario Sc#MiC_a.

Annex B – CG converges along the number of iteration

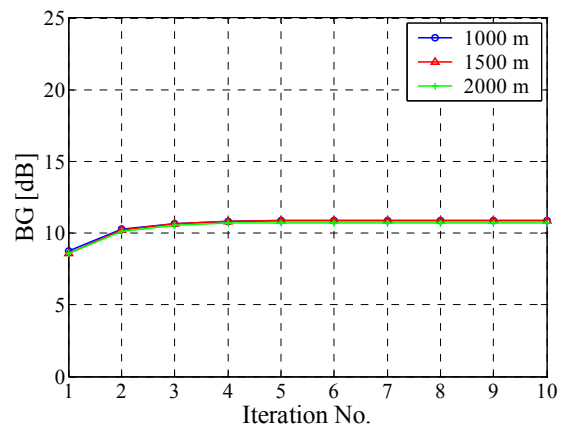
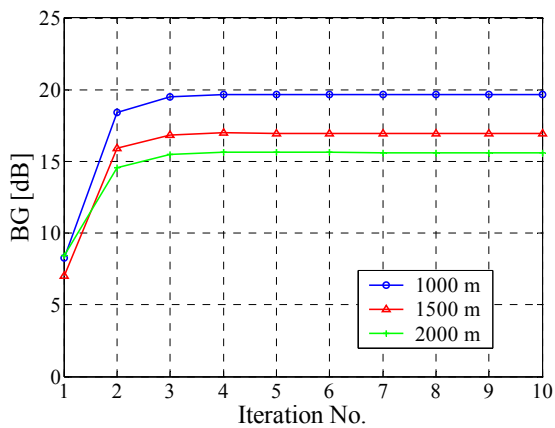
MaC; scenario Sc#MaC_a;



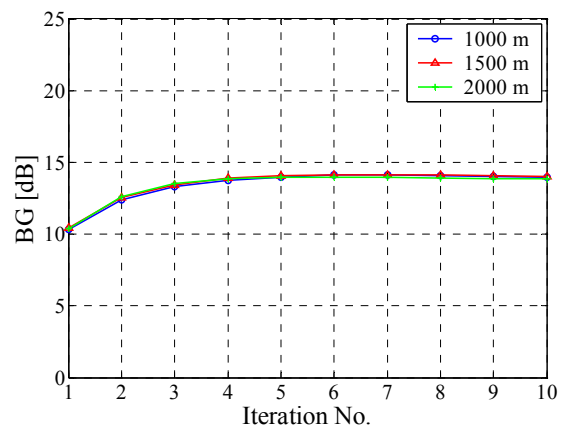
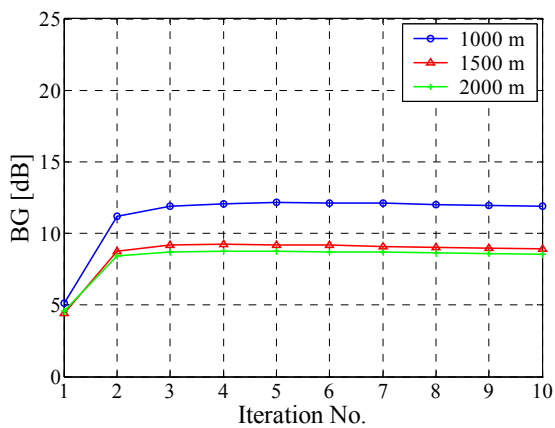
MiC; scenario Sc#MiC_a;



a) 1st step of beamforming



b) 2nd step of beamforming



c) 3rd step of beamforming

Figure B.1 – Comparison of CG converges along the number of iteration for MaC and MiC.

References

- [3GPP03a] 3GPP, *Physical layer - General description*, Technical Specification 25.201 v6.0.0, Dec. 2003 (<http://www.3gpp.org>).
- [3GPP03b] 3GPP, *Spreading and modulation (FDD)*, Technical Specification 25.213 v6.0.0, Dec. 2003 (<http://www.3gpp.org>).
- [Bagh99] Baghaie,R., “Systolic implementation of sample-by-sample conjugate gradient algorithm”, in *Proc. of FINSIG’99 – IEEE Finish Signal Processing Symposium*, Oulu, Finland, May 1999.
- [Bala97] Balanis,C.A., *Antenna Theory: analysis and design*, John Wiley & Sons, New York, USA, 1997.
- [ChKi92] Choi,S. and Kim,D.H., “Adaptive Antenna Array Utilising the Conjugate Gradient Method for Compensation of Multipath Fading in a Land Mobile Communication”, in *Proc. of VTC’92 – 42nd IEEE Vehicular Technology Conference*, Denver, CO, USA, May 1992.
- [DGVC03] Debbah,M., Gil,J.M., Venes,J., Cardoso,F., Marques,G. and Correia,L.M., *Final report on channel models*, IST-FLOWS Project, Deliverable D13, EC-IST Office, Brussels, Belgium, Sep. 2003, (<http://www.flows-ist.org>).
- [Gil04] Gil,J.M., *Dependencies of Adaptive Beamforming on the Propagation Channel in Wideband Mobile Communications*, PhD. Thesis, Instituto Superior Técnico, Technical University of Lisbon, Lisbon, Portugal, June 2004.
- [GiCo02] Gil,J.M. and Correia,L.M., *Dependence of Adaptive Beamforming Performance on Directional Channel Macro-Cell Scenarios for UMTS*, COST 273, Temporary Document TD(02)050, Espoo, Finland, May 2002.

- [GiCo03] Gil,J.M. and Correia,L.M., “Adaptive Beamforming Dependencies on Wideband and Directional Propagation Characteristics in Micro- and Macro-Cell UMTS Scenarios”, in *Proc. of PIMRC'2003 – 14th IEEE International Symposium on Personal, Indoor and Mobile Communications*, Beijing, China, Sep. 2003.
- [GiMC01] Gil,J.M., Mendez,J., and Correia,L.M., “Comparison of Recursive Least Squares and Conjugate Gradient Applied to Adaptive Beamforming in UMTS”, in *Proc. of IST Mobile Communications Summit 2001*, Barcelona, Spain, Sep. 2001.
- [Goda97] Godara,L.C., “Application of Antenna Arrays to Mobile Communications, Part II: Beam-forming and Direction-of-Arrival Considerations”, *Proc. of the IEEE*, Vol. 85, No. 8, Aug. 1997, pp. 1193-1245.
- [HeBK99] Hernandez,R.I., Baghaie,R. and Kettunen,K., “Implementation of Gram-Schmidt conjugate direction and conjugate gradient algorithms”, in *Proc. of FINSIG'99 – IEEE Finish Signal Processing Symposium*, Oulu, Finland, May 1999.
- [Hera00] Herault,L., *Project Presentation Report*, IST-ASILUM project, Deliverable D0.2, EC-IST Office, Brussels, Belgium, Apr. 2000, (<http://www.nari.ee.ethz.ch/~asilum/>).
- [HoTo01] Holma,H. and Toskala,A., *WCDMA for UMTS*, John Wiley & Sons, Chichester, UK, 2001.
- [KALN01] Kaaranen,H., Ahtiainen,A., Laitinen,L., Naghian,S. and Niemi,V., *UMTS Networks*, John Wiley & Sons, Chichester, UK, 2001.
- [LiLo96] Litva,J. and Lo,T.K., *Digital Beamforming in Wireless Communications*, Artech House, Norwood, MA, USA, 1996.
- [LiRa99] Liberti,J.C. and Rappaport,T.S., *Smart Antennas for Wireless Communications: IS-95 and Third Generation CDMA Applications*, Prentice Hall, Upper Saddle River, NJ, USA, 1999.

- [MaCo01] Marques,M.G. and Correia,L.M., “A Wideband Directional Channel Model for UMTS Micro-cells”, in *Proc. of PIMRC’01 – 12th IEEE Personal, Indoor and Mobile Radio Communications Conference*, San Diego, CA, USA, Sep. 2001.
- [Marq01] Marques,M.G., *A Wideband Directional Model for Micro-Cells in UMTS*, M.Sc. Thesis, Instituto Superior Técnico, Technical University of Lisbon, Lisbon, Portugal, 2001.
- [Olej02] Olejniczak,J., *Impact of the directional channel in adaptive beamforming for UMTS-FDD in micro-cells*, Graduation Project, Instituto Superior Técnico, Technical University of Lisbon, Lisbon, Portugal, 2002.
- [Szym02] Szymański,T., *Impact of the directional channel in adaptive beamforming for UMTS-FDD in macro-cells*, Graduation Project, Instituto Superior Técnico, Technical University of Lisbon, Lisbon, Portugal, 2002.
- [VeBu88] Van Veen,B.D. and Buckley,K.M., ”Beamforming: A Versatile Approach to Spatial Filtering”, *IEEE Acoustics, Speech and Signal Processing Magazine*, Vol. 5, No. 2, Apr. 1988, pp. 4-24.
- [ZoMa00] Zollinger,E. and Marques,G., *Wideband Directional Channel Model and Measurement Campaign*, IST-ASILUM Project, Deliverable D2.1, IST Central Office, Brussels, Belgium, Nov. 2000.